Safety and Integrity of
Arctic Marine Pipelines

Progress Report #3
Centrifuge Test PR3d-2 Report

Submitted to:

Minerals Management Service
United States Department of the Interior

Submitted by:

C-CORE
St. John's, Newfoundland

C-CORE

The correct citation for this report is :

Phillips, R., Hurley, S. and King, T. (1998). "Safety and Integrity of Arctic Marine Pipelines; Progress Report #3 - Centrifuge Test PR3d-2 Report." Contract Report for Minerals Management Service, United States Department of the Interior, C-CORE Publication 98-C8, June.

Clients:	Minerals Management Service United States Department of the Interior
Project:	
Client's Contract Ref.:	
C-CORE Cost Center:	3-40425
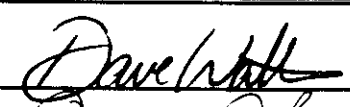
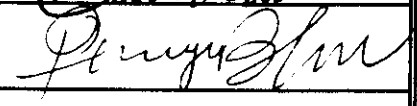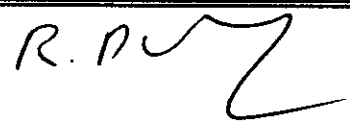|	
Document Title:	Safety and Integrity of Arctic Marine Pipelines Progress Report #3 - Centrifuge Test PR3d-2 Report
C-CORE Pub. No.:	98-C8
Prepared By:	Ryan Phillips, Shawn Hurley, Tony King
Date:	May, 1998
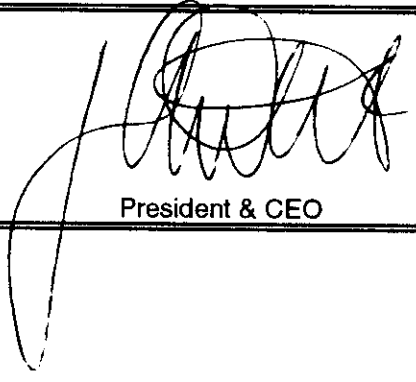
Reviewers	Document Accepted	
	Date	Signature
Technical Accuracy	29 May May 29/98	Dave White
Syntax	June 5/98	Eleanor Hoskitt
Layout & Presentation	June 5/98	E. Hoskitt
General Evaluation	3 June 98	R. P

Approval for Release	
Date:	President & CEO

TABLE OF CONTENTS

1.0   INTRODUCTION

The Pressure Ridge Ice Scour Experiment (PRISE) is an ongoing jointly funded, international, multiphase program. The goal is to develop the capability to design pipelines and other seabed installations in regions scoured by ice, taking into account the soil deformations and stress changes within the soil which may be caused during a scouring event. The need for this capability was identified during a round-table discussion with several oil companies and federal government representatives in 1990 during an international workshop on ice scour held in Calgary.

Pipelines on Arctic seafloors in the U.S.A., Russia and Canada are in danger of being damaged by the action of sea ice pressure ridge keels that scour the seafloor. Oil and gas pipelines must be buried below the maximum expected scour depth to avoid direct ice/pipeline interaction which would cause serious damage to the pipe. However, just as soil at the seabed surface is subject to large scour-induced displacements, the soil beneath a scouring keel also moves. These sub-scour deformations also must be taken into account as they may cause unacceptable shear and bending stresses in a buried pipeline.

A safe burial depth must be selected to ensure pipeline safety and integrity in areas affected by ice scouring. The safe burial depth will not be the same for every region of the seafloor. This is dependant on three factors: (1) the maximum expected depth of ice-scouring, which will determine the absolute minimum top-of-pipe depth of burial; (2) the soil type and condition which will affect the response of sub-scour soils to ice induced stresses, and (3) the mechanism of load transfer from the deforming soil to the buried pipe. Thus the problem of pressure ridge ice scouring is, for each case, to determine a safe burial depth that not only will avoid direct ice/pipeline interaction, but also will minimize the risk of damage due to sub-scour soil movements.

This report presents the results of the second centrifuge test conducted as part of PRISE Phase 3d. The experiment was conducted at 1:10 scale, thus centrifugal acceleration at the base of the model keel was set to 10g. The attack angle was 30 degrees and the target scour depth was 7.5 mm. The model testbed was prepared using a sandy-silt obtained from a local quarry, hereafter referred to as Capital Silt. An additional scour was preformed at 1-g for comparison with the 10-g scour.

1

2.0   RESEARCH OBJECTIVES

The principal objective of the work being conducted for the MMS is to examine the magnitude and extent of sub-scour deformations in a dilatant soil. This information is essential to achieve the PRISE goal of designing pipelines and other seabed installations for regions scoured by ice, and to take into account the soil deformations and stress changes which may be caused during a scour event.

The objective will be achieved through four activities:

(1)   Direct field observation of sub-scour deformations under fresh ice scours in compact silt in a tidal estuary. This is documented in Paulin (1997).

(2)   Simulation of full scale or field ice scour events by two centrifuge modelling experiments;

(3)   Development of the existing numerical model to predict sub-scour deformation profiles in dilatant materials; and

(4)   Assist in developing the MMS Alaskan workshop on indigenous knowledge in technology.

This work is being carried out as part of Phase 3d of PRISE. This report addresses the second centrifuge modelling test of activity (2). Activities (1) and (4) have been completed. Activity (3) is currently underway.

3.0 MODEL PREPARATION

Model preparation began Monday, April 13/1998. The model seabed was prepared from Capital Silt with the properties listed in Table 1. A grain size curve is shown in Figure 1.

Table 1.   Properties of Capital Silt

Mean grain size (D_{50})	0.064 mm
Effective grain size (D_{10})	0.015 mm
D_{60}	0.078 mm
D_{30}	0.037 mm
Uniformity coefficient (C_u)	5.2
Coefficient of curvature (C_c)	1.17

A 292 mm thick layer of No. 00 silica sand was first placed in the strongbox to serve as a drainage layer. Once this layer was compacted and levelled, an extrusion plate was placed on top of it to allow removal of the sample for post-test examination. This extrusion plate was covered with a layer of geotextile and the marker grids were put into position prior to placement of the Capital Silt. The marker grids were constructed by glueing together a grid of spaghetti strands. A total of 16 vertical strands were spaced at 15 mm and short pieces of lead solder, 4 mm long, were glued to these strands at spacings of 15 mm. Horizontal spaghetti strands with a spacing of 30 mm were employed to complete the grid. The grid was mounted on a plastic base which was, in turn, taped to the geotextile layer. Figure 2 shows the placement of the grids during the addition of the Capital Silt. A total thickness of 133 mm of capital silt was dumped in the strongbox. The spaghetti strands softened once they were in contact with the wet silt and might be considered to have no impact on the behaviour of the silt during the scouring events. Pore pressure transducers were positioned in the Capitol Silt under the scour paths. The surface of the silt was levelled and the package was loaded on the centrifuge and spun under 10-g to consolidate. The excess pore pressures and the settlement of the silt during the consolidation stage are shown in Figure 3. Once this step was complete, the horizontal drive and the keel were positioned for the scour. The layout of the assembled package is shown in Figure 4.
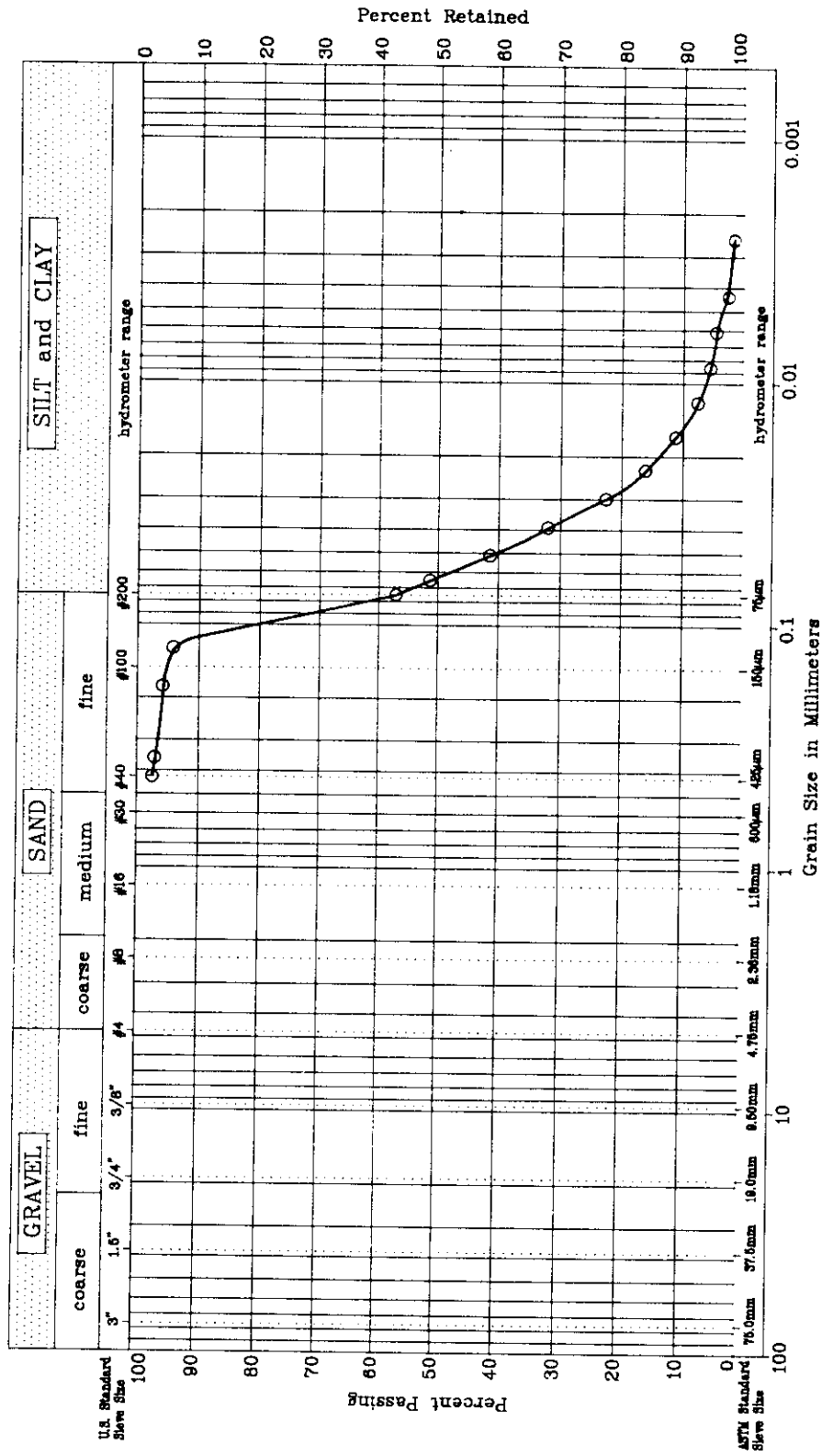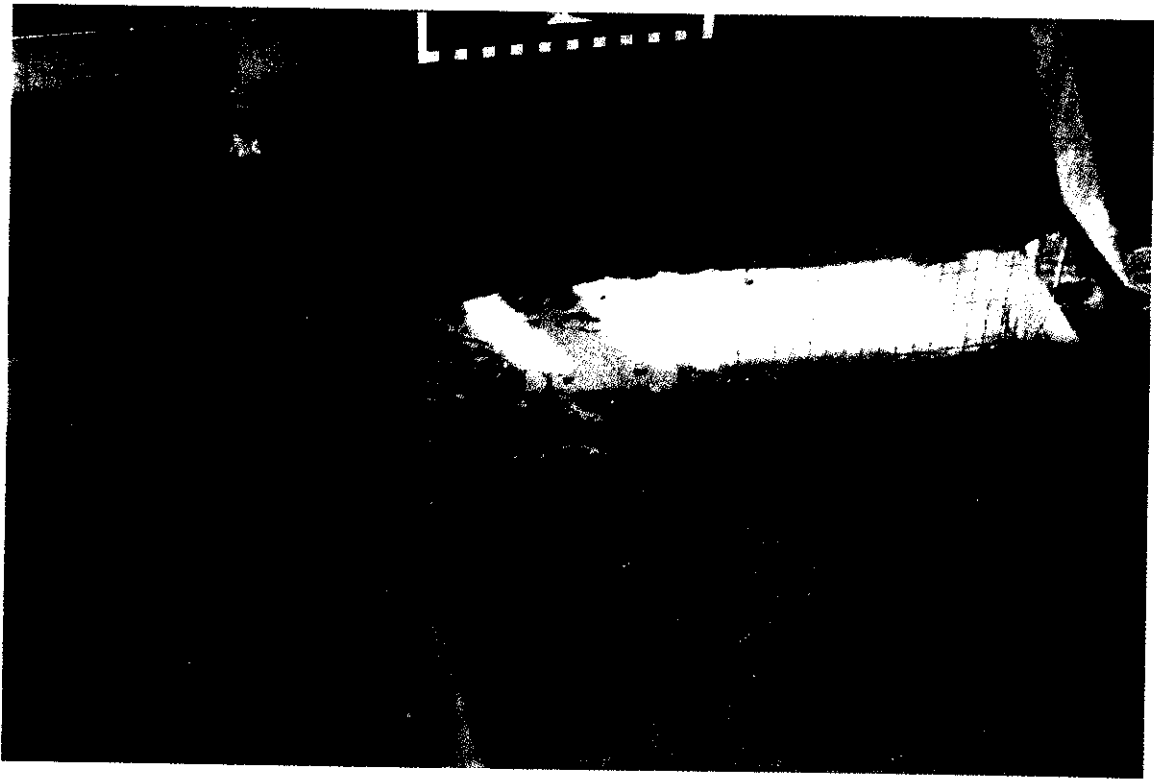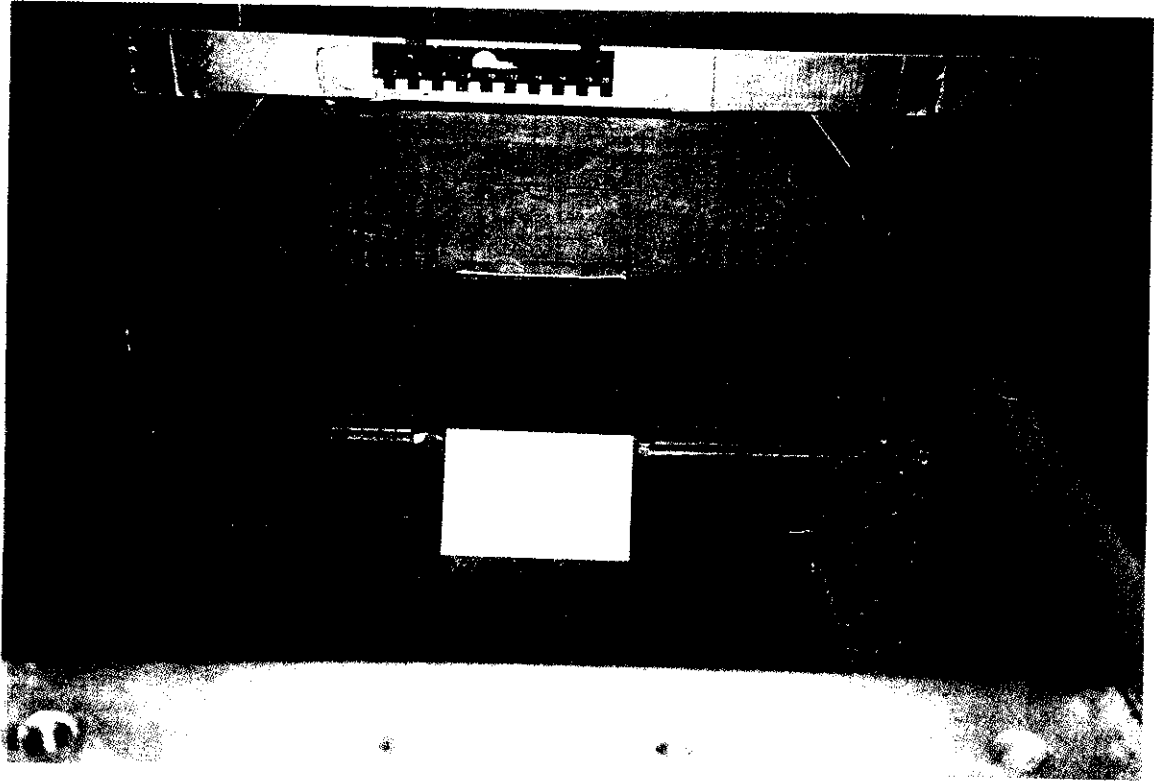
GRAIN SIZE DISTRIBUTION
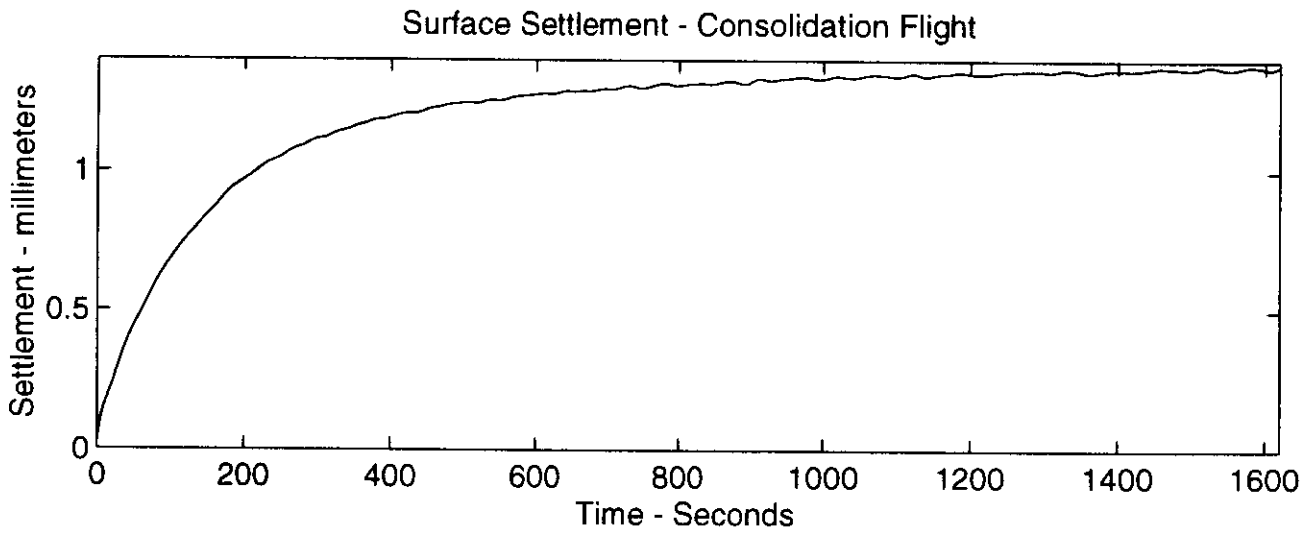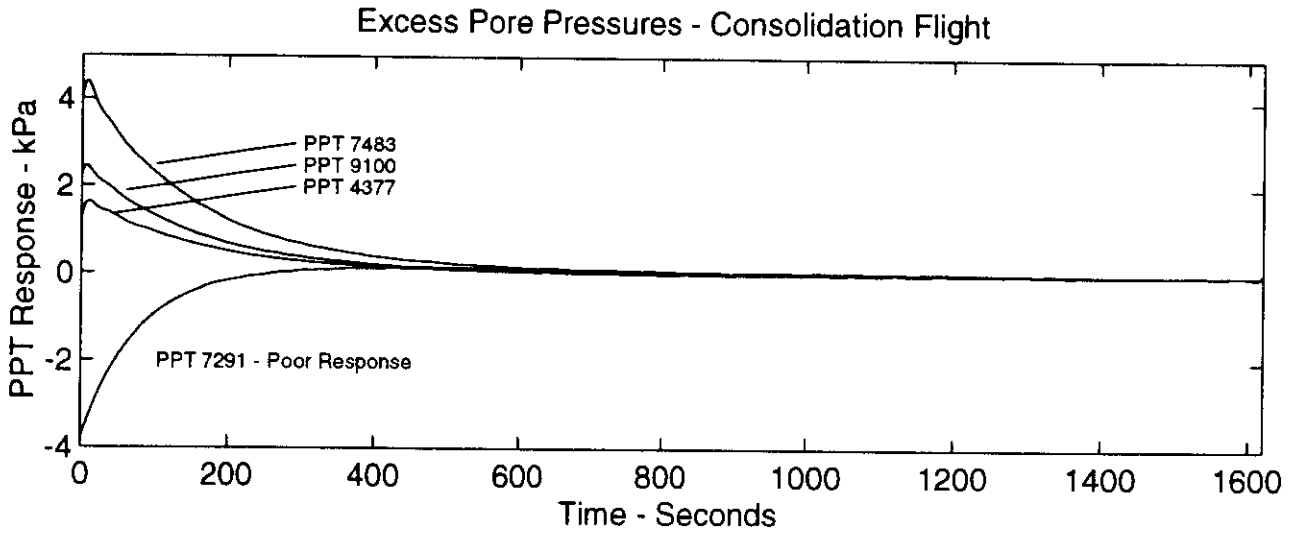

Sample Description: Capital Silt

$D_{10} = 0.015mm$ $D_{30} = 0.037mm$ $D_{60} = 0.078mm$ $C_U = 5.2$ $C_C = 1.17$

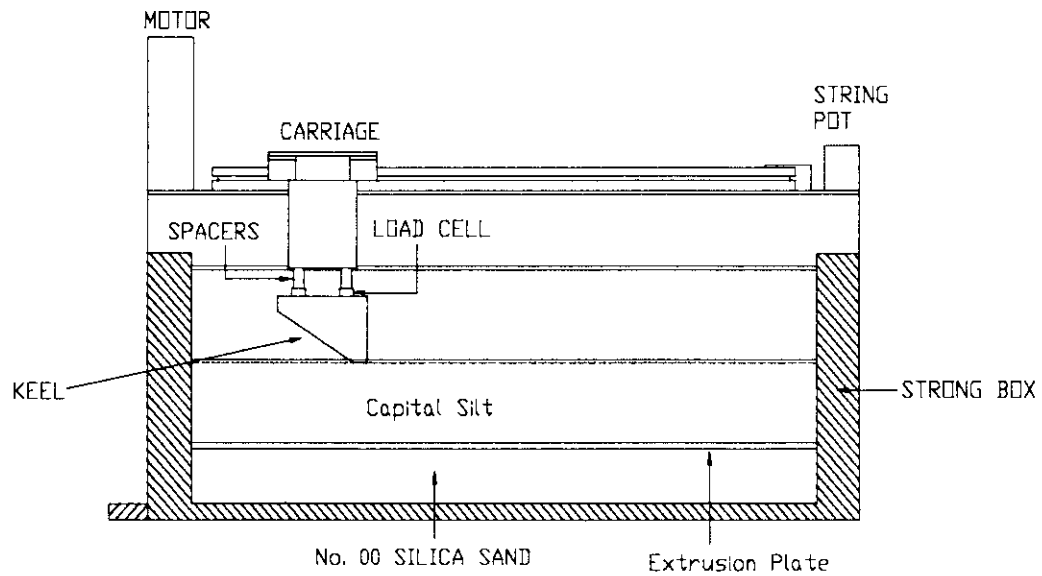|	Grain Size Curve Capital Silt	FIGURE 1

4

Placement of Spaghetti Grids During Addition of Capital Silt

FIGURE 2

Excess Pore Pressures and Settlement During Consolidation Flight

FIGURE 3

TENSION CELL

STRING POT

RAILS

DRIVE UNIT

1/8" CABLES

1100

CARRIAGE
ASSEMBLY

STRONG BOX

SIGNAL
CONDITIONING
BOX

CAMERA
ASSEMBLY

1410

MOTOR

STRING
POT

CARRIAGE

SPACERS

LOAD CELL

KEEL

STRONG BOX

Capital Silt

No. 00 SILICA SAND

Extrusion Plate
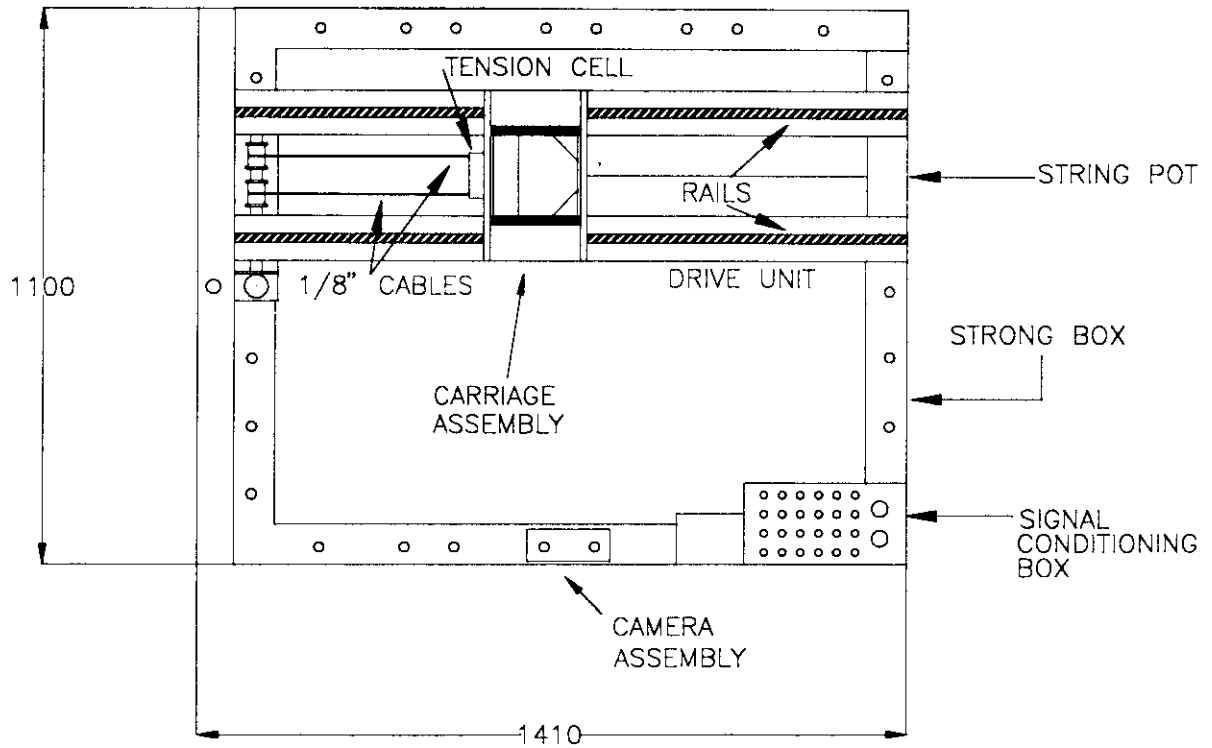
PRISE TEST PACKAGE CROSS-SECTION

| C-CORE | Layout of Assembled Package | FIGURE 4 |

4.0 INSTRUMENTATION AND DATA ACQUISITION

Table 2 provides a summary of the instrumentation used in centrifuge test PR3d-2. In total, 16 active transducers were employed, including instrumentation used to measure the vertical and horizontal loads acting on the keel, contact pressures acting on the model keel, keel displacement, and excess pore pressures generated during the scour events. Figure 5 shows the locations of the transducers which were attached to the model keel.

Table 2.   Electronic Instrumentation

Device	Identification	Measured or Derived Quantity
Pore Pressure Transducer	PPT 9100	Pore pressure under 10-g scour
Pore Pressure Transducer	PPT 7291	Pore pressure under 10-g scour
Pore Pressure Transducer	PPT 4377	Pore pressure under 1-g scour
Pore Pressure Transducer	PPT 7483	Pore pressure under 1-g scour
Tension Cell	TC04A	Model horizontal force
Tension Cell	TC04B	Model horizontal force
Load Cell	LC394469	Model vertical force / keel front
Load Cell	LC513034	Model vertical force / keel front
Load Cell	LC394580	Model vertical force / keel rear
Load Cell	LC490203	Model vertical force / keel rear
Pressure Transducer	PT423117	Contact pressure / horizontal base
Pressure Transducer	PT423107	Contact pressure / inclined surface
Pressure Transducer	PT517931	Contact pressure / inclined surface
Pressure Transducer	PT504863	Contact pressure / inclined surface
String Potentiometer	SP02	Model horizontal position
Displacement Transducer	LDT12	Sand surface settlement

Video cameras were also mounted on the strongbox to allow observation of the test.

8
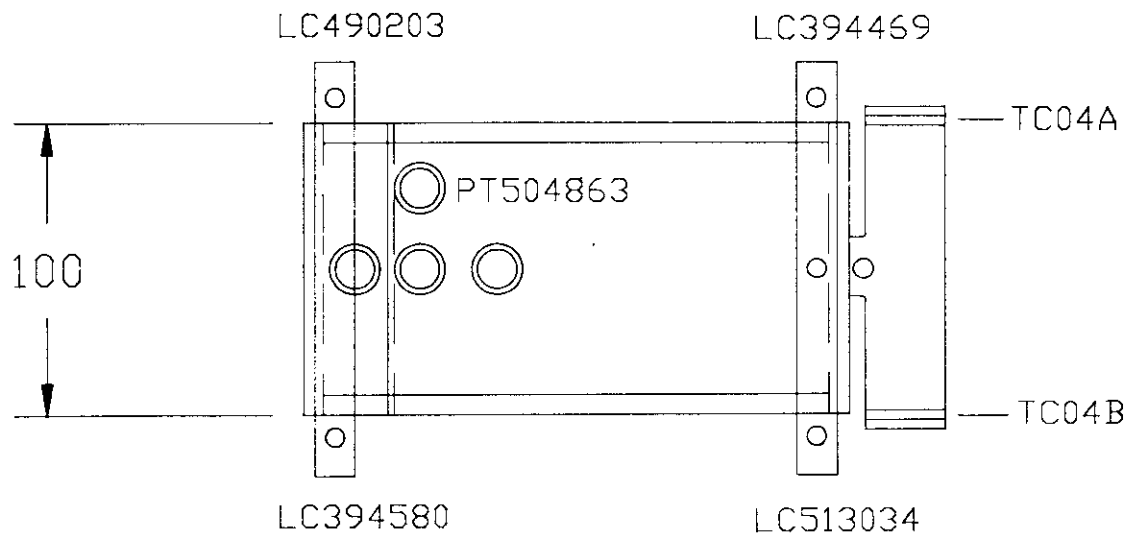
PLAN
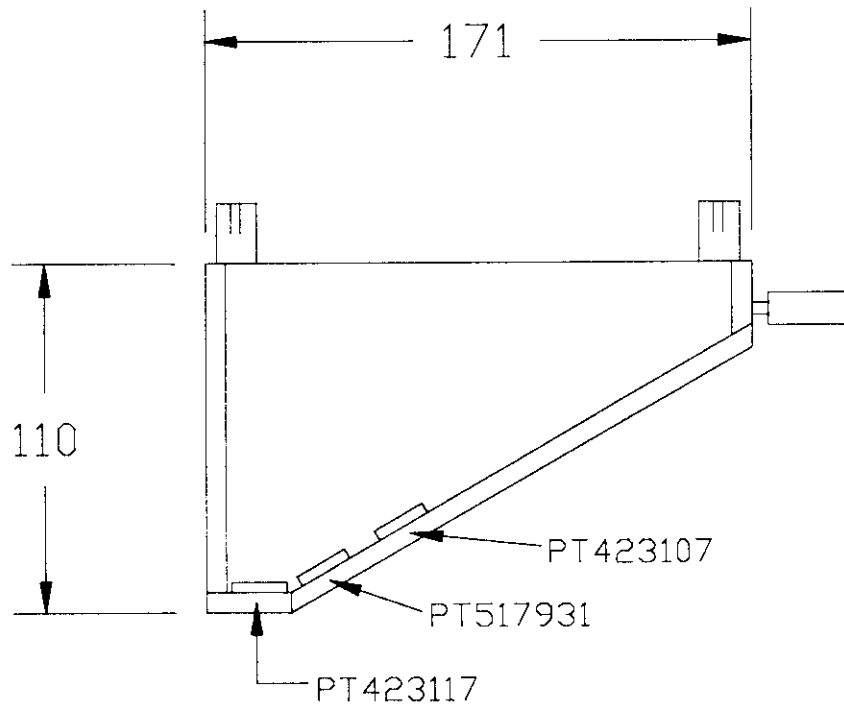
PROFILE

|	Location of Transducers on Model Keel	FIGURE 5

5.0   CENTRIFUGE TEST PR3D-2

Centrifuge test PR3d-2 was conducted on Friday, April 22, 1998. This test consisted of two scour events, the first performed at 10-g and the second at 1-g.   Both tests were performed in the same test package. Once the 10-g scour was complete and the centrifuge stopped, the horizontal drive was repositioned so that a second scour could be performed parallel to the first at 1-g.

5.1 10-g Model Scour Event

For the 10-g scour the centrifuge was operated at a speed of 41.5 rpm, to induce 10-g at the bottom of the model keel. Data acquired during the scouring event included measurement of resultant forces and contact pressures acting on the model keel, keel displacement and pore pressures generated in the Capital Silt during the scour event.

Figure 6 shows the keel displacement plotted versus time during the 10-g scouring event, as determined from measurements of the string potentiometer (SP02) which was attached to the carriage assembly. This data record was used to evaluate the horizontal position of the model keel in presentation of the results for each of the other transducers. The actual keel velocity or scour rate was 110.7 mm/s, equal to the slope of the displacement-time curve.
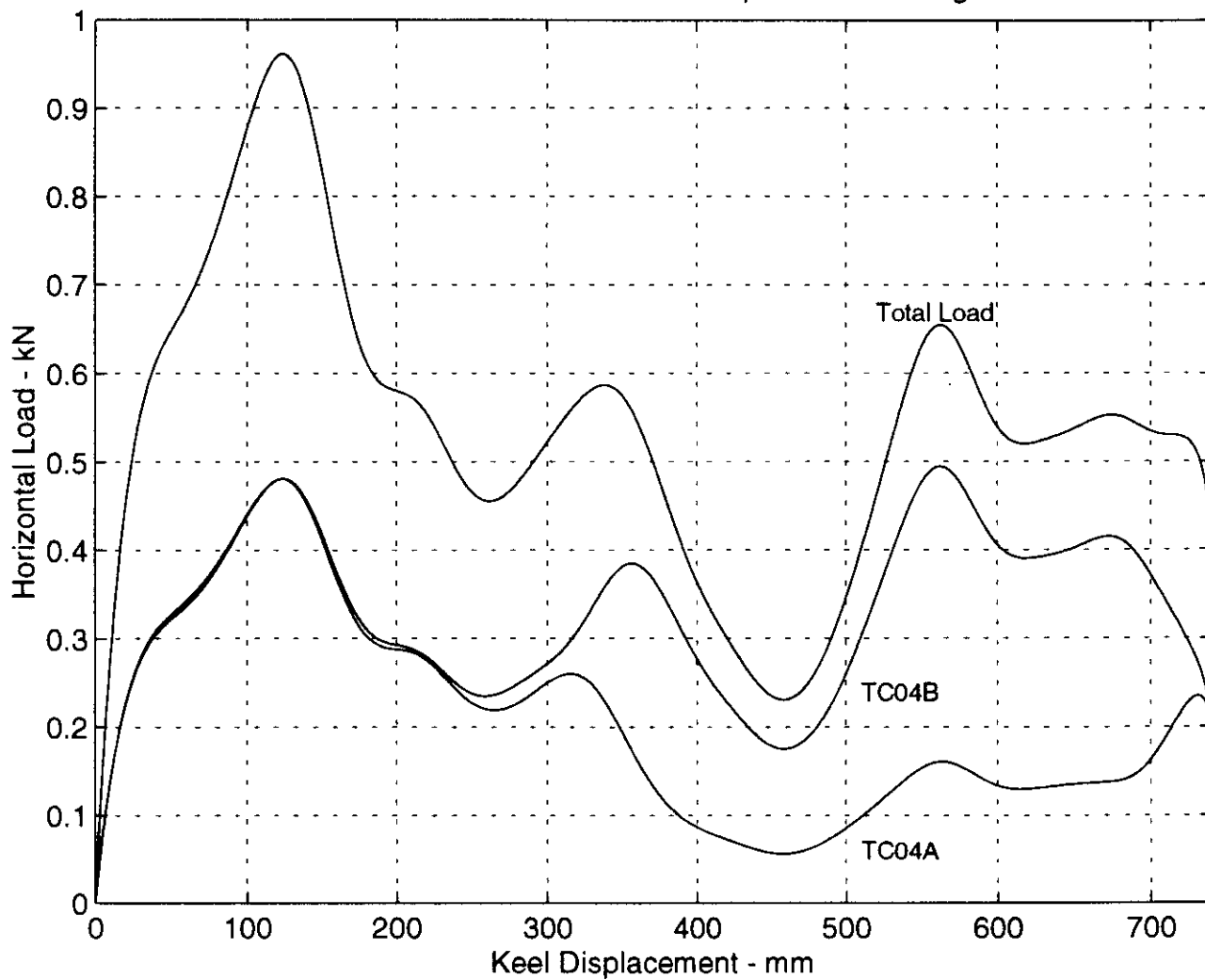
The total horizontal force was computed through summation of contributions from individual tension load cells (TC04A and TC04B) located at the connection between the drive system pulling cables and the model keel. Figure 7 shows the horizontal force for each tension cell and the total horizontal force plotted against keel displacement during the scour event. Steady state conditions were achieved after about 250 mm of keel displacement. The total average horizontal force imposed under steady state conditions was approximately 0.45 kN at model scale (or 45 kN at prototype scale). The oscillation in the forces after steady state is partly attributable to the unevenness of the mudline.

Keel Displacement vs. Time - 10-g Test

Mean Speed: 110.7 mm/s, T=1 to 7 seconds
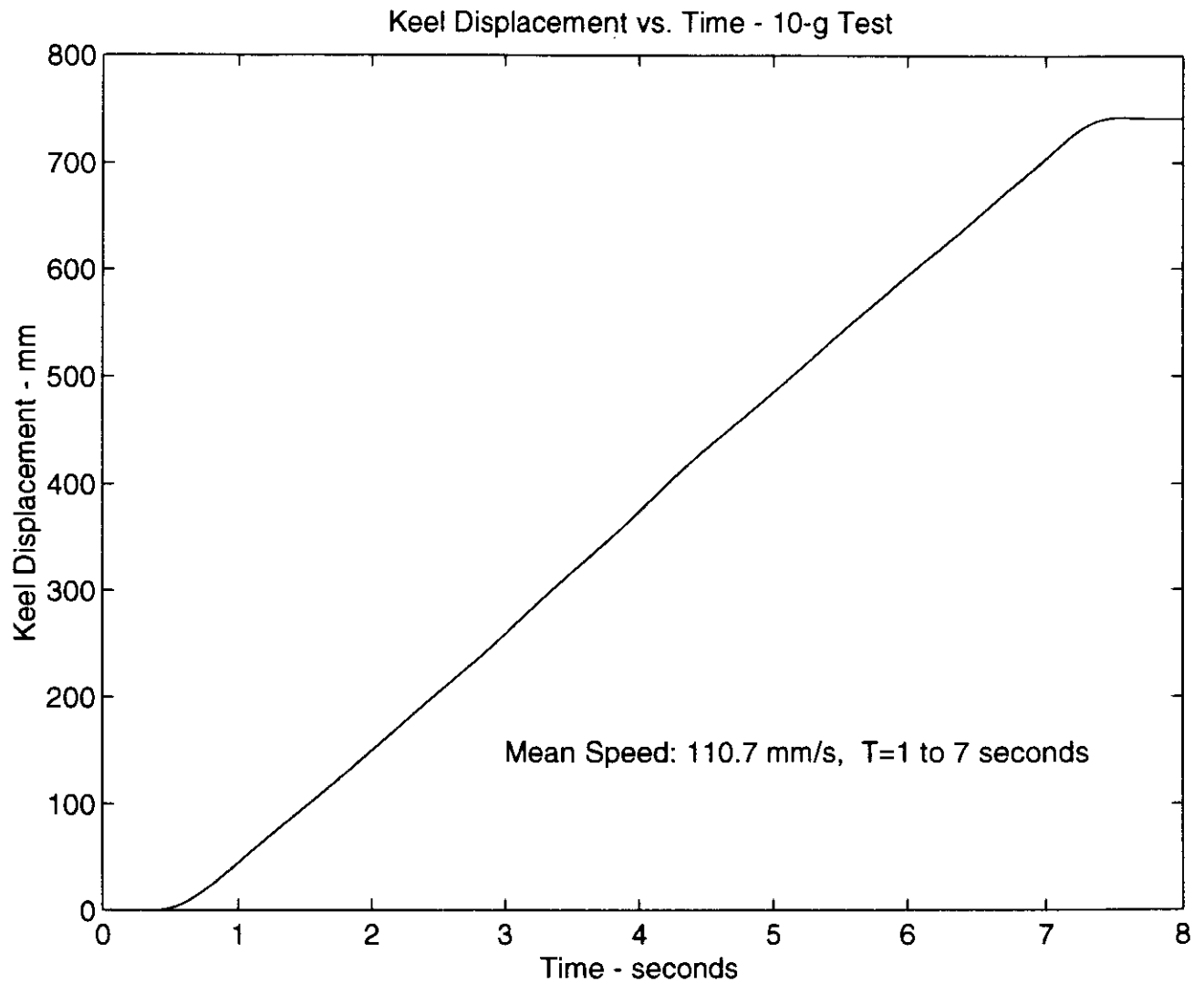
| | Keel Displacement During 10-g Scour Event | FIGURE 6 |

Model Horizontal Force vs. Keel Displacement - 10-g Test

Horizontal Forces During
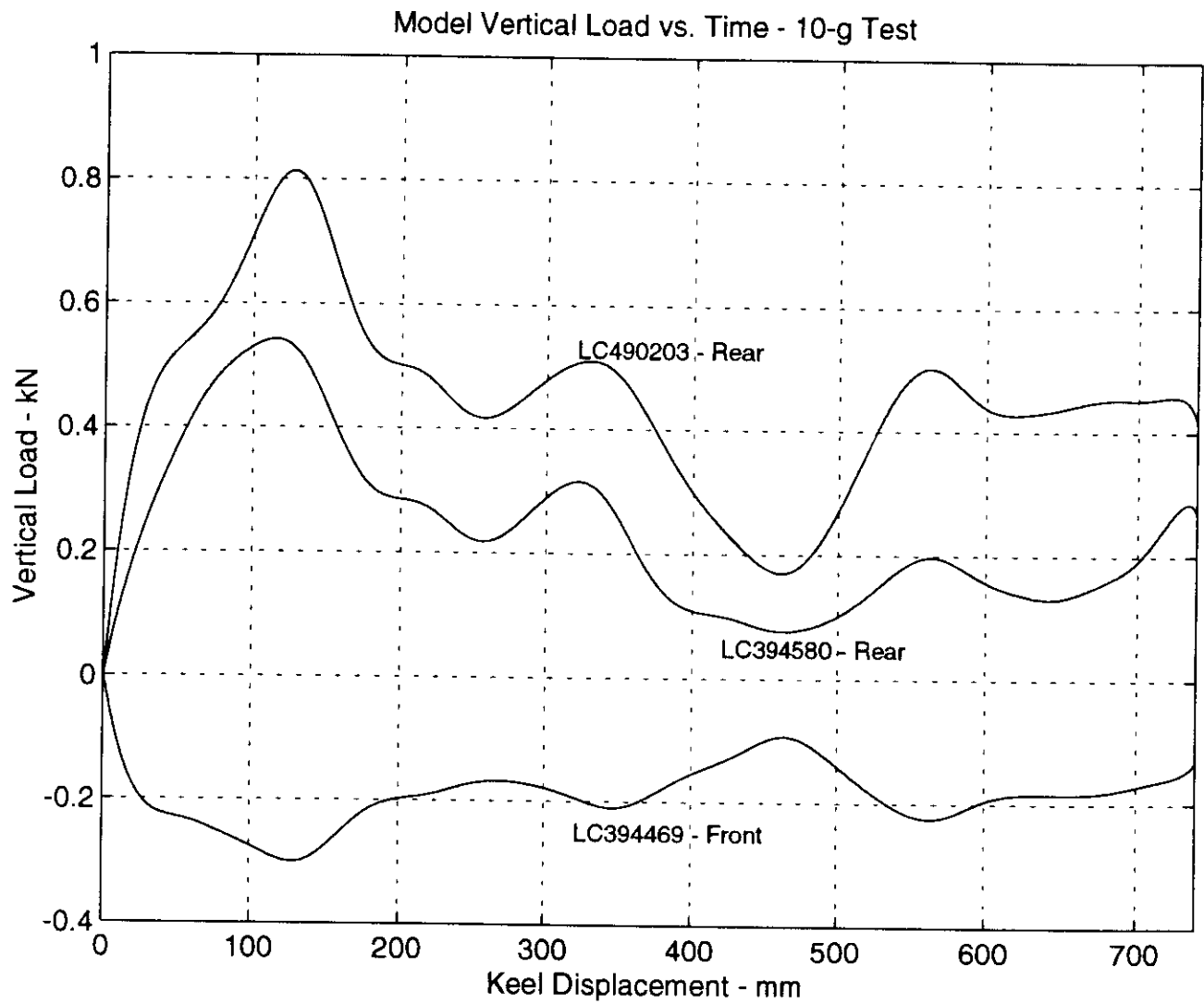10-g Scour Event

FIGURE
7

The total vertical force was evaluated through summation of the responses of the tension/compression load cells (LC394469, LC394580, and LC490203) which linked the model keel to the carriage assembly. Load cell LC513034 malfunctioned during this test and no data are available for plotting. Figure 8 shows the measured vertical force from the three functioning load cells, plotted against keel displacement during the scour event. It can be seen that the rear load cells are in compression while the front one is in tension. Steady state was achieved after approximately 250 mm. The relative magnitudes of the loads measured by the three functioning load cells are quite similar to those observed in test PR3d-1 (Hurley and Phillips, 1998). Since load cells LC513034 and LC394580 had very similar output levels during PR3d-1, the assumption was made that the same thing occurred during this test. This implies an average, steady state, vertical force of 0.58 kN (or 58 kN at prototype scale).
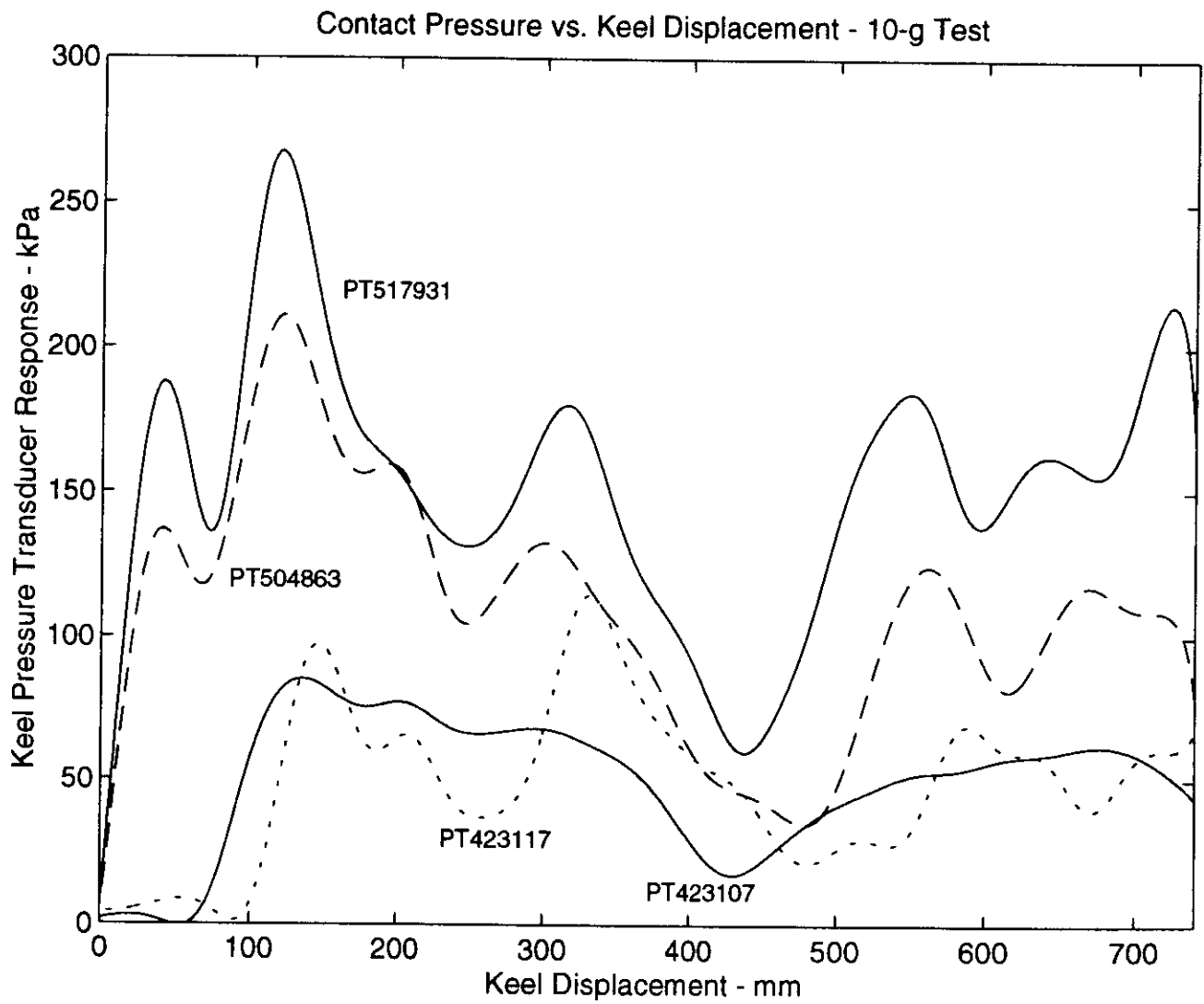
The contact pressures developed during the scouring event are displayed in Figure 9 which presents the data records for the four interface pressure transducers (PT423107, PT517931, PT423117, and PT504863) mounted on the model keel. The pressure record for the transducer located at the horizontal base of the keel (PT423117) indicated an average response over the duration of the event of approximately 44 kPa. The two pressure transducers located on the lower positions of the inclined face of the keel (PT517931 and PT504863) displayed average responses of 132 and 88 kPa. The transducer located on the upper position of the inclined face (PT423107) exhibited a response of approximately 44 kPa.

Two pore pressure transducers (PPT 9100 and PPT 7291) were located under the 10-g scour and the response of these transducers is shown in Figure 10. PPT 9100 shows the development of a suction of approximately -27 kPa during the scour event. The weak response of PPT 7291, which also showed an anomalous response during the consolidation flight, is probably not indicative of the actual pore pressures experienced during the scour.
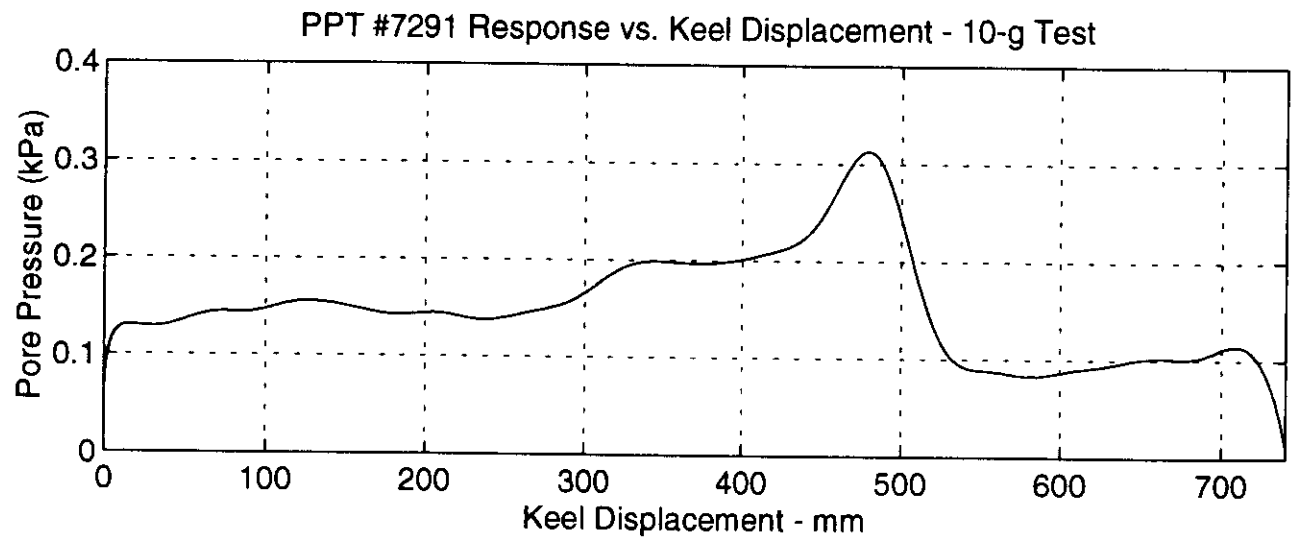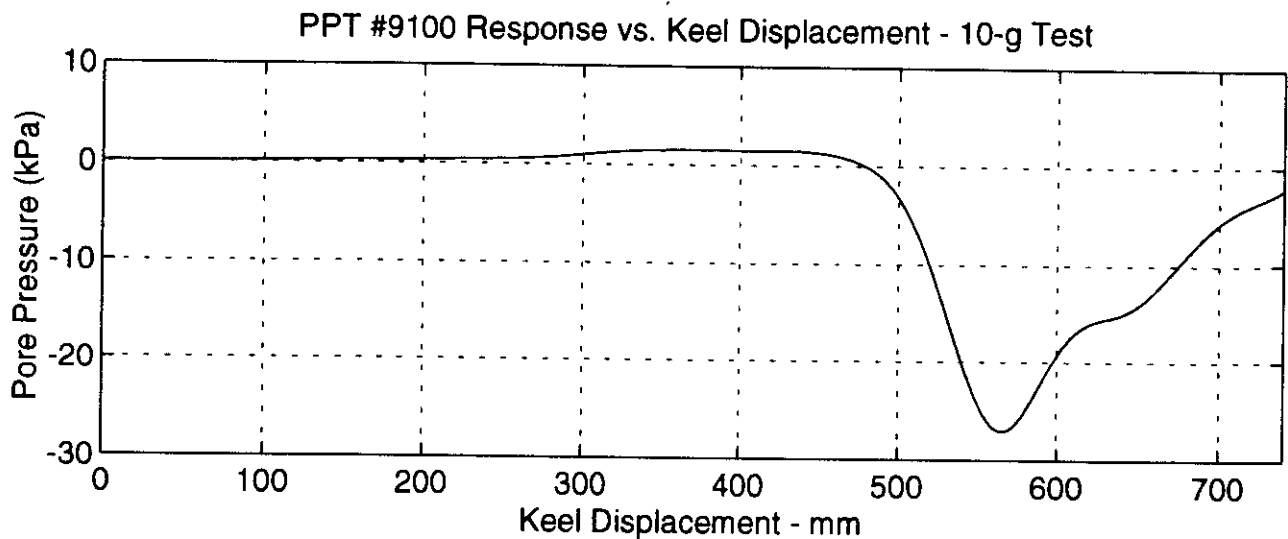
13

Model Vertical Load vs. Time - 10-g Test

LC490203 - Rear

LC394580 - Rear

LC394469 - Front

Vertical Load - kN

Keel Displacement - mm

Vertical Forces During 10-g Scour Event

FIGURE 8

C-CORE

Contact Pressure vs. Keel Displacement - 10-g Test

PT517931

PT504863

PT423117

PT423107

Keel Pressure Transducer Response - kPa

Keel Displacement - mm

Contact Pressures During 10-g Scour Event

FIGURE 9

PPT #9100 Response vs. Keel Displacement - 10-g Test

PPT #7291 Response vs. Keel Displacement - 10-g Test

|	Excess Pore Pressures During 10-g Scour Event	FIGURE 10

5.2 1-g Scour Event

After the 10-g scour was complete the centrifuge was stopped and the horizontal drive was repositioned to allow a second scour to be conducted at 1-g. Approximately three hours elapsed between the time the centrifuge was stopped and the 1-g scour was conducted. The package was left on the arm of the centrifuge during the 1-g test, allowing the same data acquisition system to be utilized for this test. Data acquired during the 1-g test included measurement of resultant forces and contact pressures acting on the model keel, keel displacement and pore pressures generated during the test.

Figure 11 shows the keel displacement plotted versus time during the 1-g scouring event, as determined from measurements of the string potentiometer (SP02) which was attached to the carriage assembly. The actual keel velocity or scour rate was 111.9 mm/s, equal to the slope of the displacement-time curve.

The total horizontal force was computed through summation of contributions from individual tension load cells (TC04A and TC04B) located at the connection between the drive system pulling cables and the model keel. Figure 12 shows the horizontal force for each tension cell and the total horizontal force plotted against keel displacement during the scour event. Steady state conditions were achieved after about 350 mm of keel displacement. The average horizontal force imposed under steady state conditions was approximately 0.68 kN.
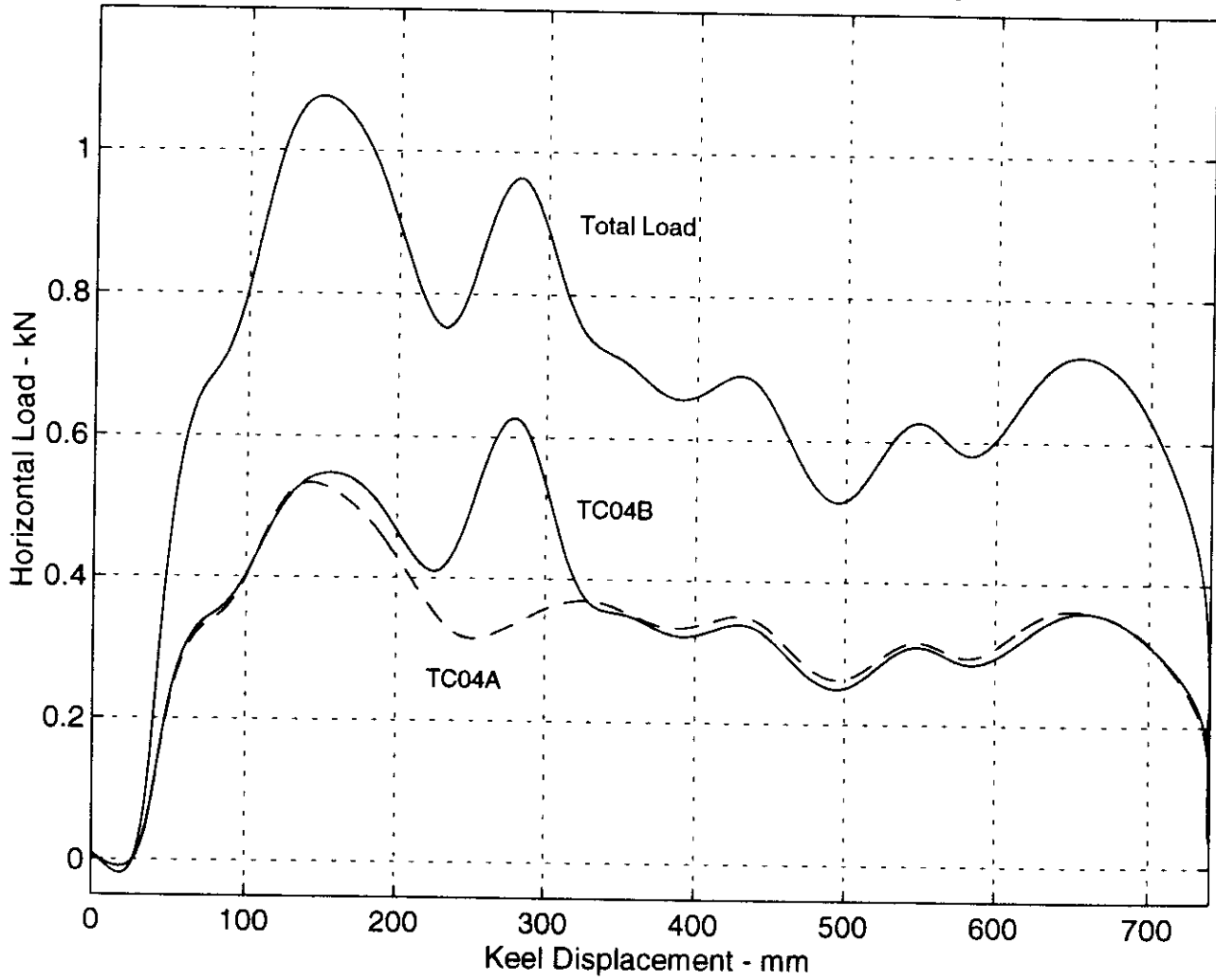
The total vertical force was evaluated through summation of the responses of the tension/compression load cells (LC394469, LC394580, and LC490203) which linked the model keel to the carriage assembly. Load cell LC513034 malfunctioned during this test and no data are available for plotting. Figure 13 shows the measured vertical force from the three functioning load cells, plotted against keel displacement during the scour event. It can be seen that the rear load cells are in compression while the front one is in tension. Steady state was achieved after approximately 350 mm. The relative magnitudes of the loads measured by the three functioning load cells is quite similar to that observed in test PR3d-1 (Hurley and Phillips, 1998). Since load cells LC513034 and LC394580 had very similar output levels during PR3d-1, the assumption was made that the same
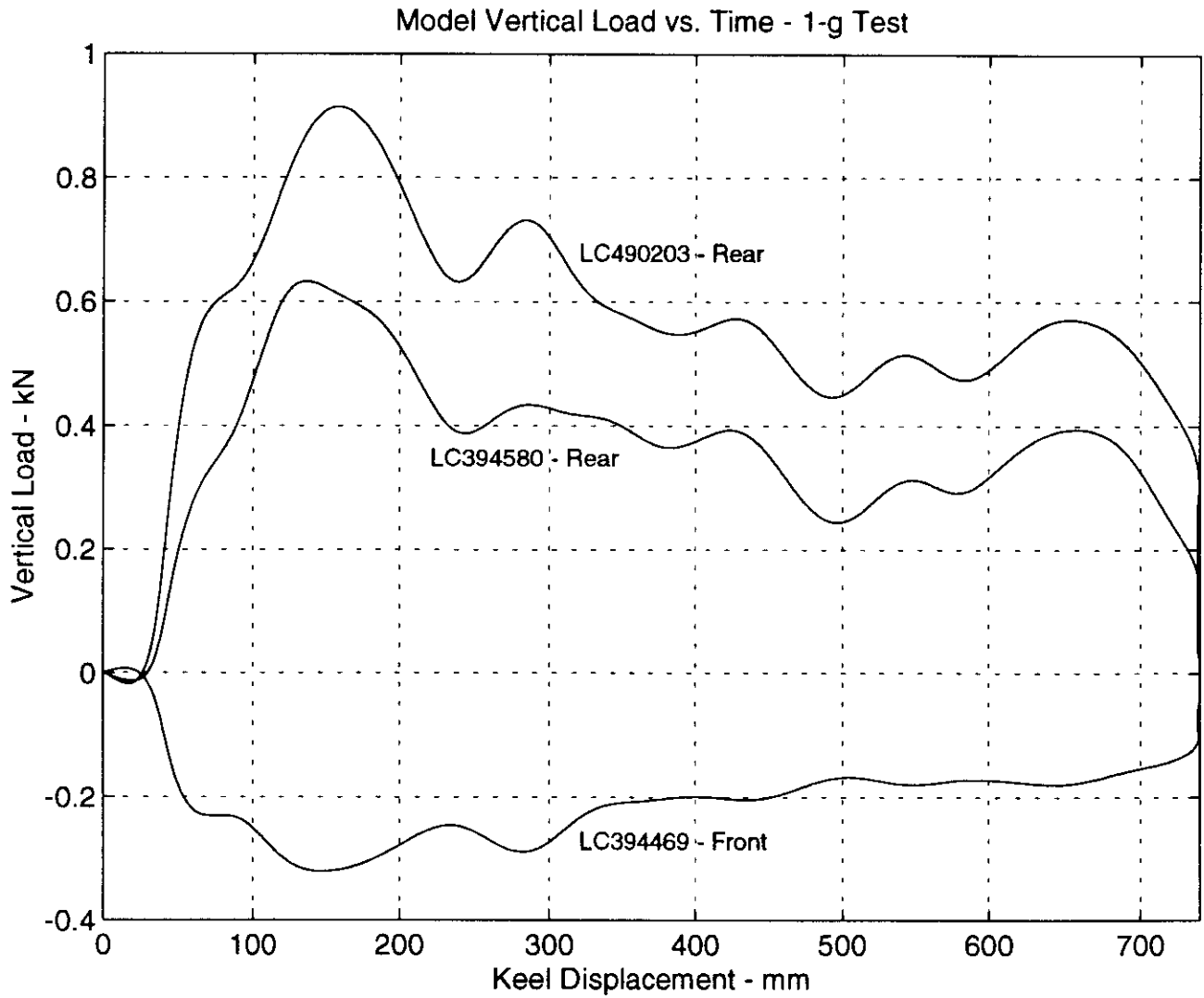
17

Keel Displacement vs. Time - 1-g Test

Mean Speed: 111.9 mm/s, T=1.5 to 7.5 seconds
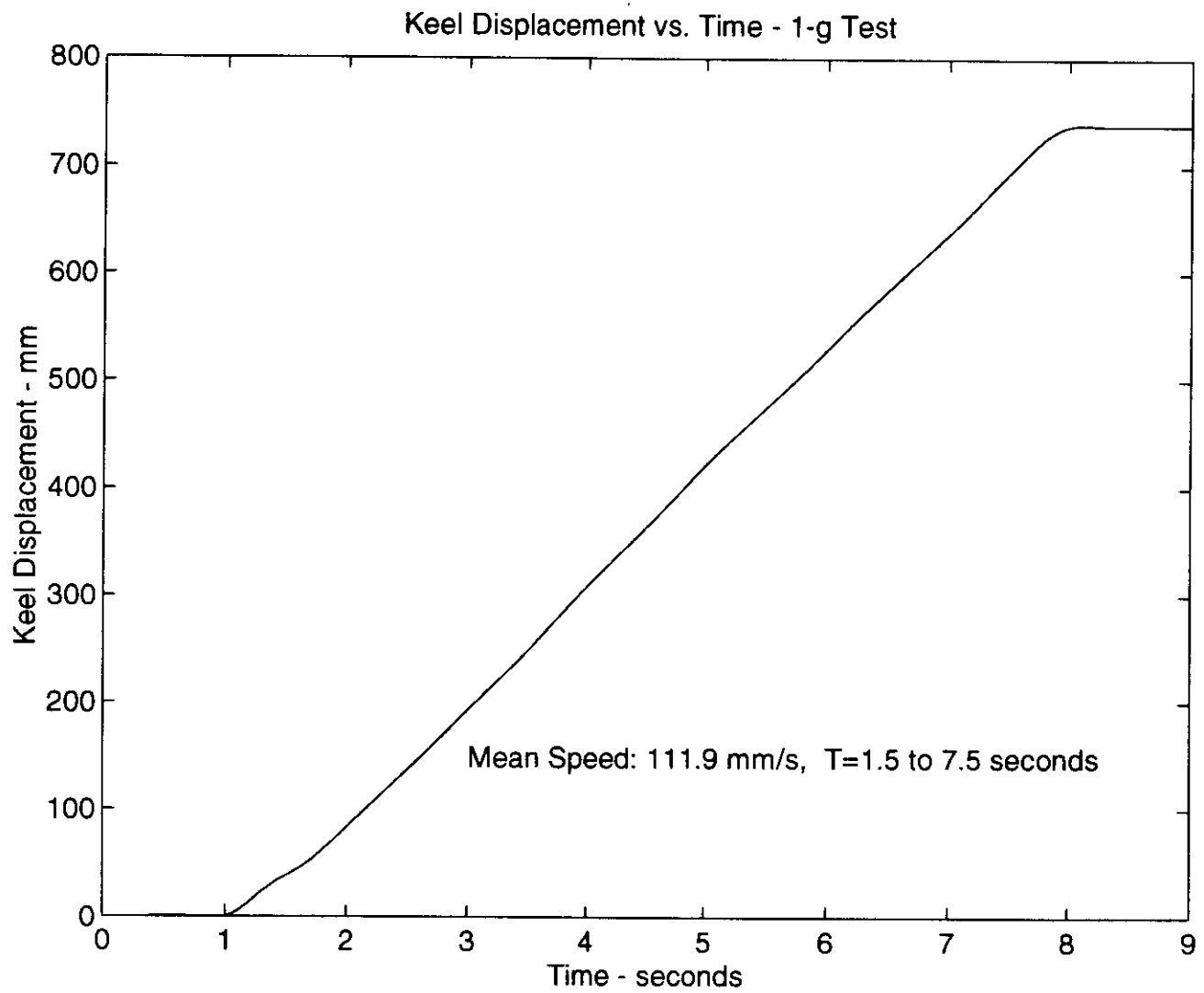
	Keel Displacement During 1-g Scour Event	FIGURE
C-CORE		11

18

Model Horizontal Force vs. Keel Displacement - 1-g Test

Total Load

TC04B

TC04A

Horizontal Load - kN

Keel Displacement - mm

| | Horizontal Forces During 1-g Scour Event | FIGURE 12 |

C-CORE

Model Vertical Load vs. Time - 1-g Test

LC490203 - Rear

LC394580 - Rear

LC394469 - Front

Vertical Load - kN

Keel Displacement - mm

C-CORE

**Vertical Forces During
1-g Scour Event**

FIGURE

13

thing occurred during this test. This implies an average, steady state, vertical force of 1.02 kN.

The contact pressures developed during the 1-g test are displayed in Figure 14 which presents the data records for the four interface pressure transducers (PT423107, PT517931, PT423117, and PT504863) mounted on the model keel. The pressure record for the transducer located at the horizontal base of the keel (PT423117) indicated an average response over the duration of the event of approximately 71 kPa. The two pressure transducers located on the lower positions of the inclined face of the keel (PT517931 and PT504863) displayed average responses of 239 and 140 kPa. The transducer located on the upper position of the inclined face (PT423107) exhibited a response of approximately 67 kPa.

Two pore pressure transducers (PPT 4377 and PPT 7483) were located under the 1-g scour and the response of these transducers is shown in Figure 15. PPT 7483 shows the development of a suction of approximately -23 kPa during the scour event. PPT 4377 over-ranged during this test, therefore the data obtained from this instrument have been omitted.
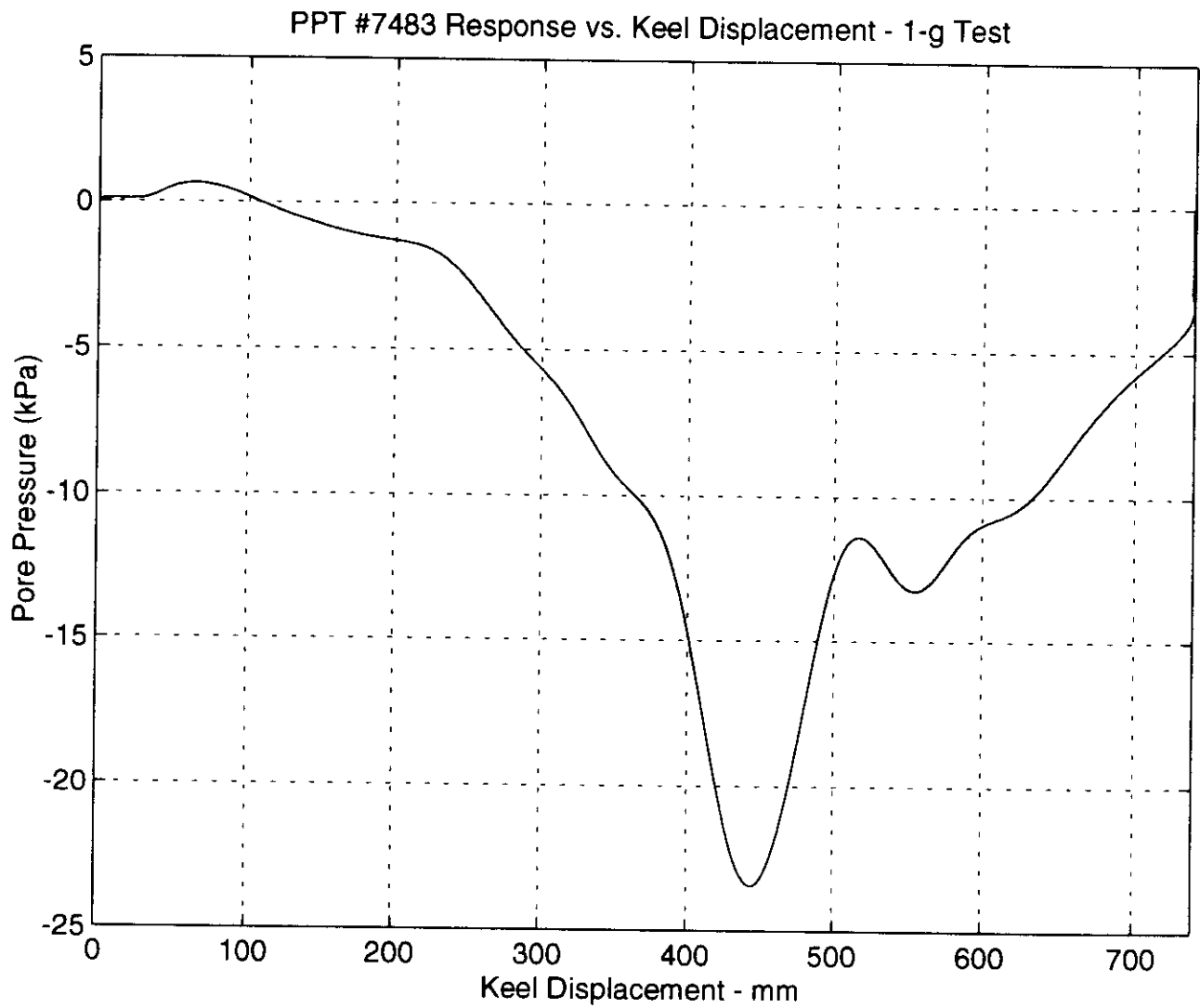
5.3 Post-Test Soil Testing

After the tests were completed and the package was unloaded, the shear vane tests and water content tests were conducted. Three shear vane tests were conducted using a 19 mm diameter hand vane. Shear strengths of 9.0, 10.5 and 9.0 kPa were obtained (mean = 9.5 kPa). However, observation of the sample and experience indicated that these shear vane measurements underestimated the shear strength of the Capital Silt and that shear strengths in the vicinity of 40 kPa would be more appropriate. Three samples were taken to determine the water content of the Capital Silt. Values of 22%, 21.5% and 20.5% were obtained (mean = 21.3%). Assuming 100% saturation and soil grains with a specific gravity(G_s) of 2.65, this indicates a soil density of 2055 kg/m^3.

Contact Pressure vs. Keel Displacement - 1-g Test

	Contact Pressures During	FIGURE
C-CORE	1-g Scour Event	14

PPT #7483 Response vs. Keel Displacement - 1-g Test
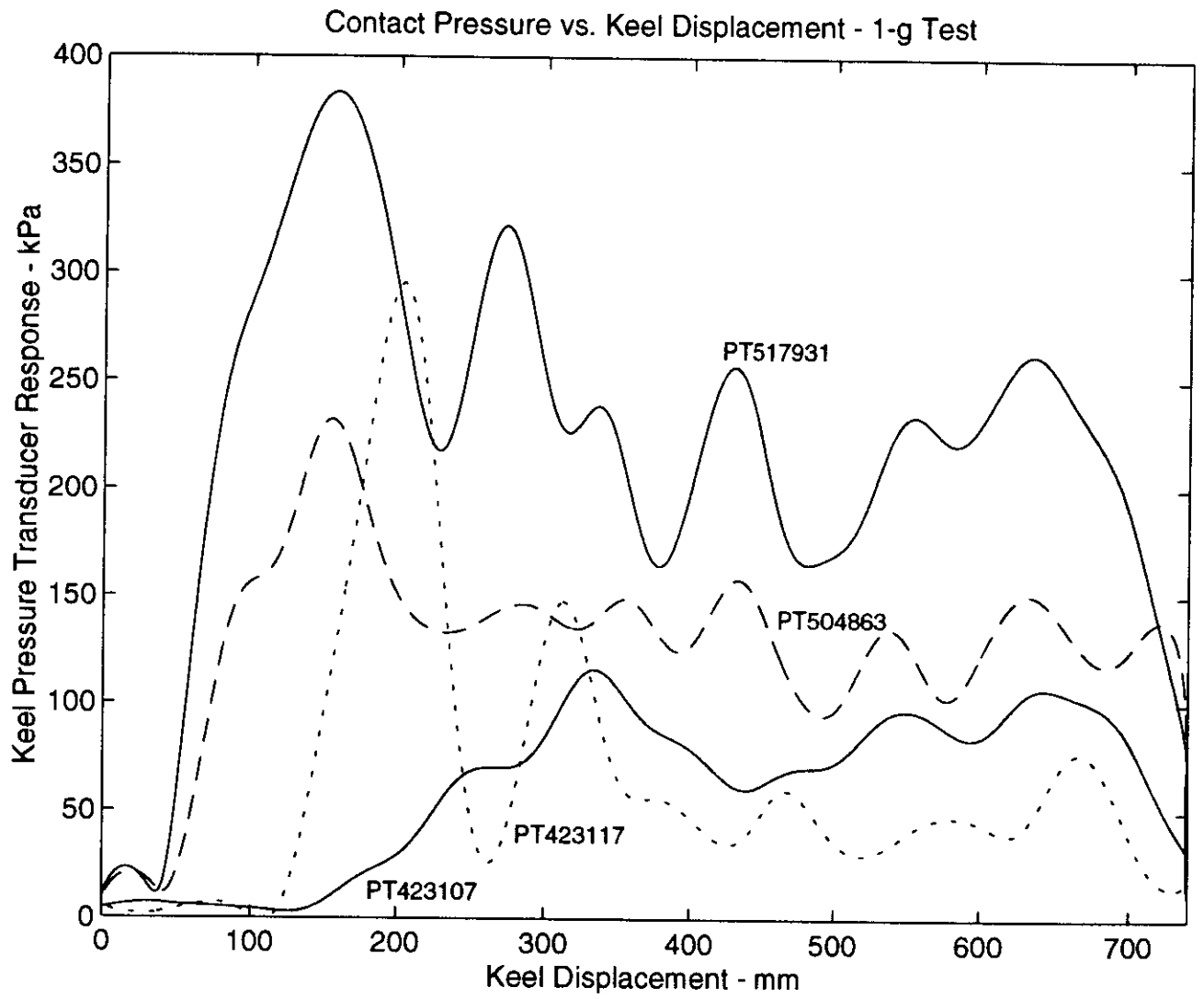
Excess Pore Pressure During
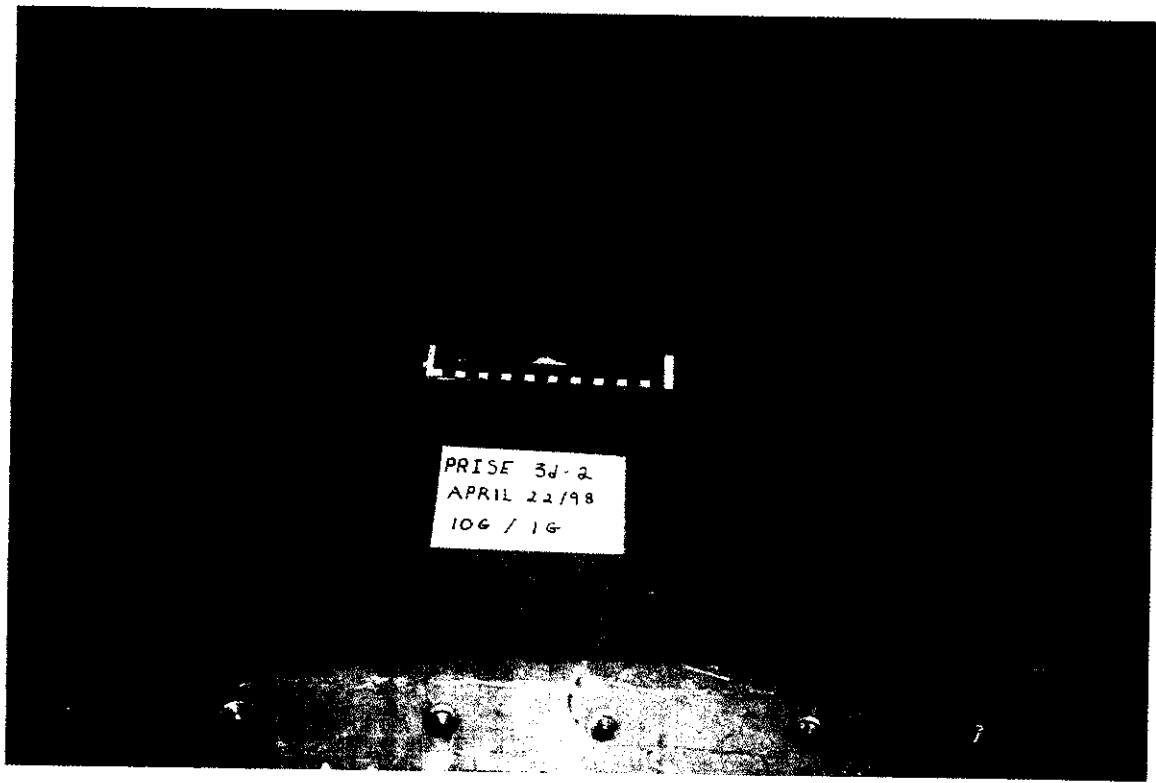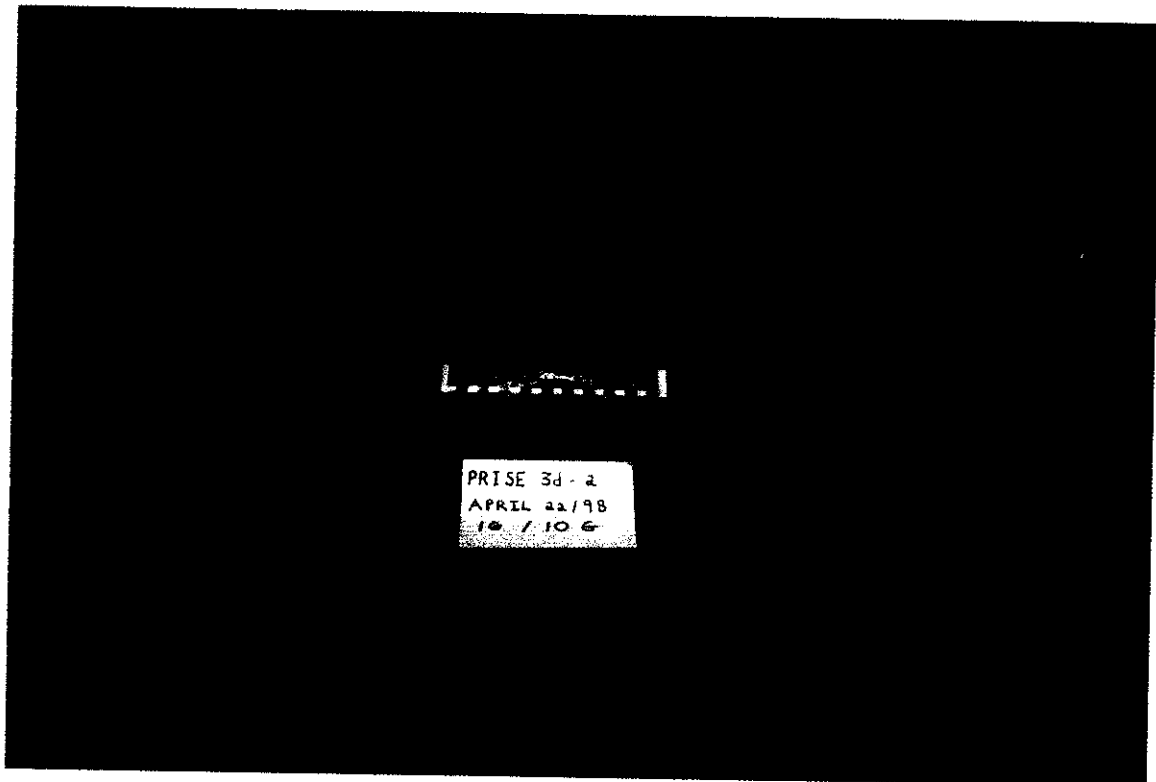1-g Scour Event

FIGURE

15

C-CORE

6.0   INVESTIGATION OF SOIL DEFORMATION

Post-test investigation of the silt testbed included photographic documentation and visual inspection of scour morphology, profiling of the scoured surface, and examination of sub-scour effects through excavation, measurement and photography of the buried displacement markers. Photographs which display two different views of each of the scours are presented in Figures 16 and 17. Profiles of the deformed sand surface were acquired using C-CORE's laser profiling system. Once the profiling was complete the sample was lifted from the strongbox using the extrusion plate. The sample was then excavated and the portions of the sample containing the marker grids were isolated and x-rayed, as shown in Figures 18 and 19. Once this process was complete, the spaghetti strands were exposed by carefully removing the silt. Photographs of the deformed grids are shown in Figures 20 and 21.

6.1 Surface Profiles

The locations of the profiles are shown in Figure 22 and the cross-sectional profiles obtained along the scours are presented in Figures 23 through 29, beginning at y-coordinate equal to 190 mm from wall of the strongbox. The scour depths at each profile location are presented in Table 3.

It is immediately evident that the scour depths for the two tests were not the same. The average depth of the 10-g scour is 3.7 mm and the average depth of the 1-g scour is 5.9 mm. Since the elevation of the keel with respect to the strongbox is fixed, this can only be attributed to an uneven sample surface. The two lateral grids (normal to the scour direction) are at y=450 (10-g) and y=447 (1-g). The centerline marker grids, parallel to the direction of the scour and directly underneath them, range in position from y=672 to y=912 for the 10-g scour and y=670 to y=910 for the 1-g scour.
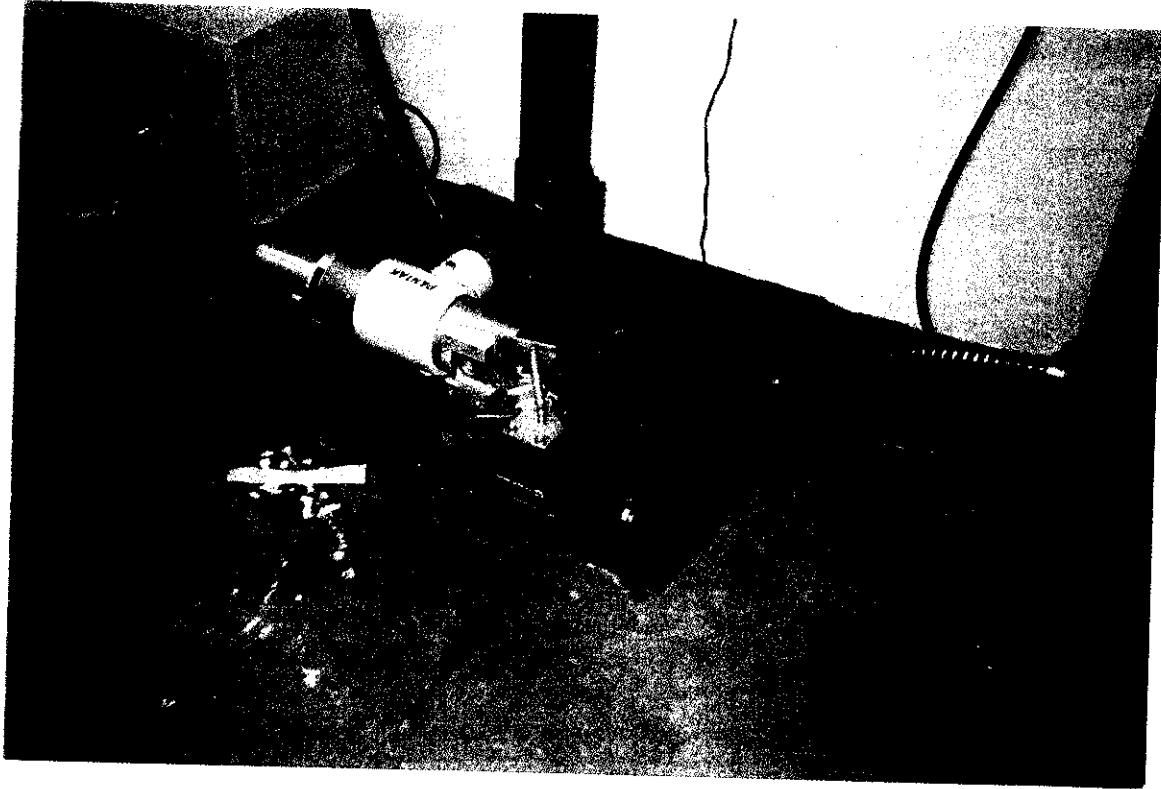
24

| | Photographs of 10-g and 1-g Scours | FIGURE 16 |

PRISE 3d - 2
10 G SCOUR
APRIL 22/98

PRISE 3d - 2
1 G SCOUR
APRIL 22/98
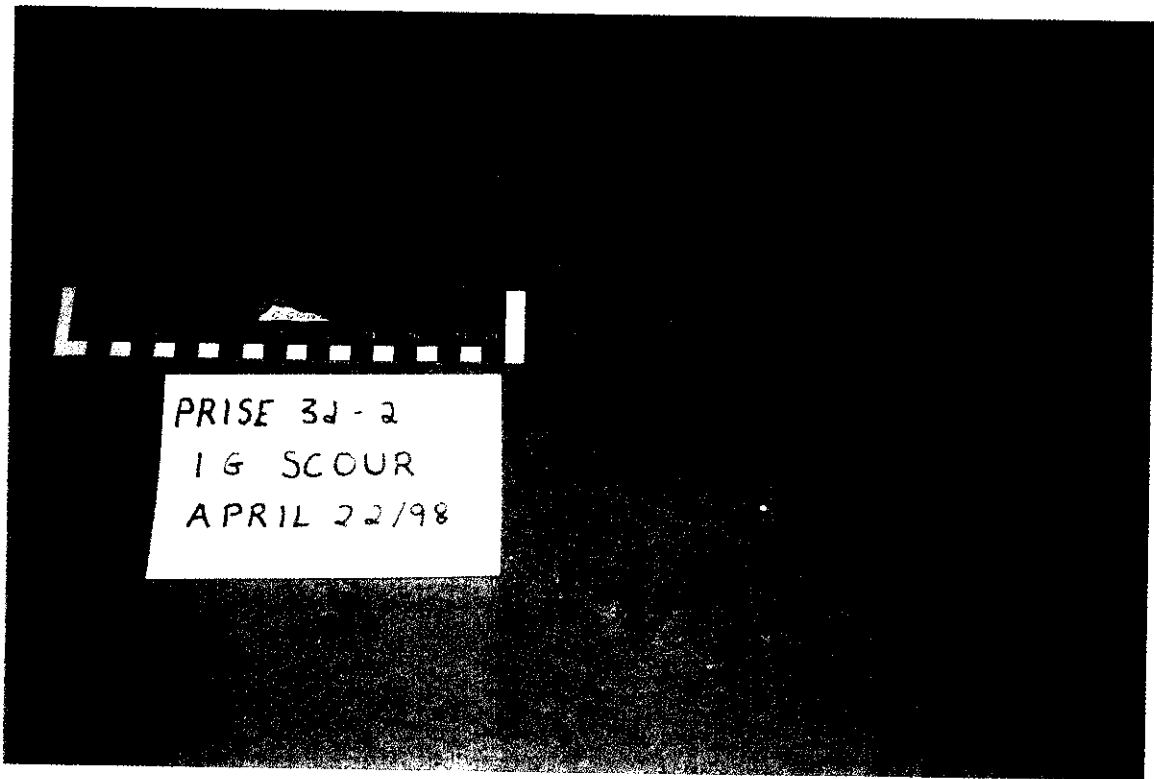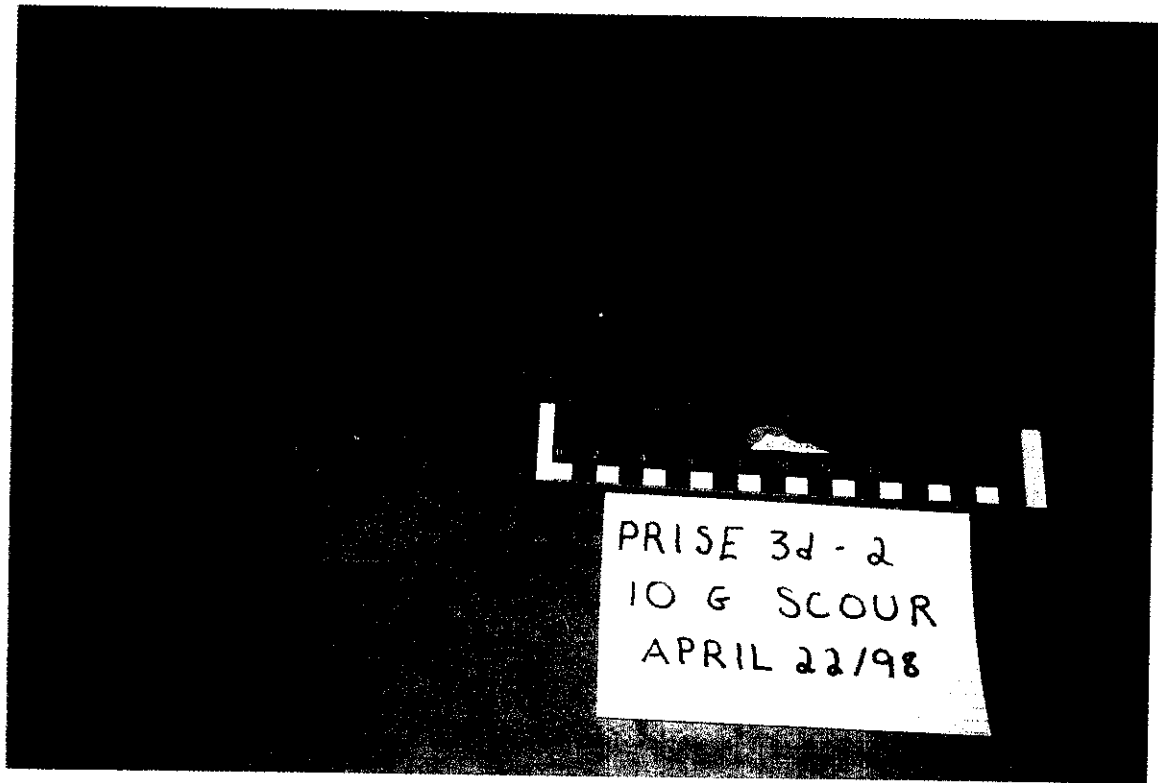
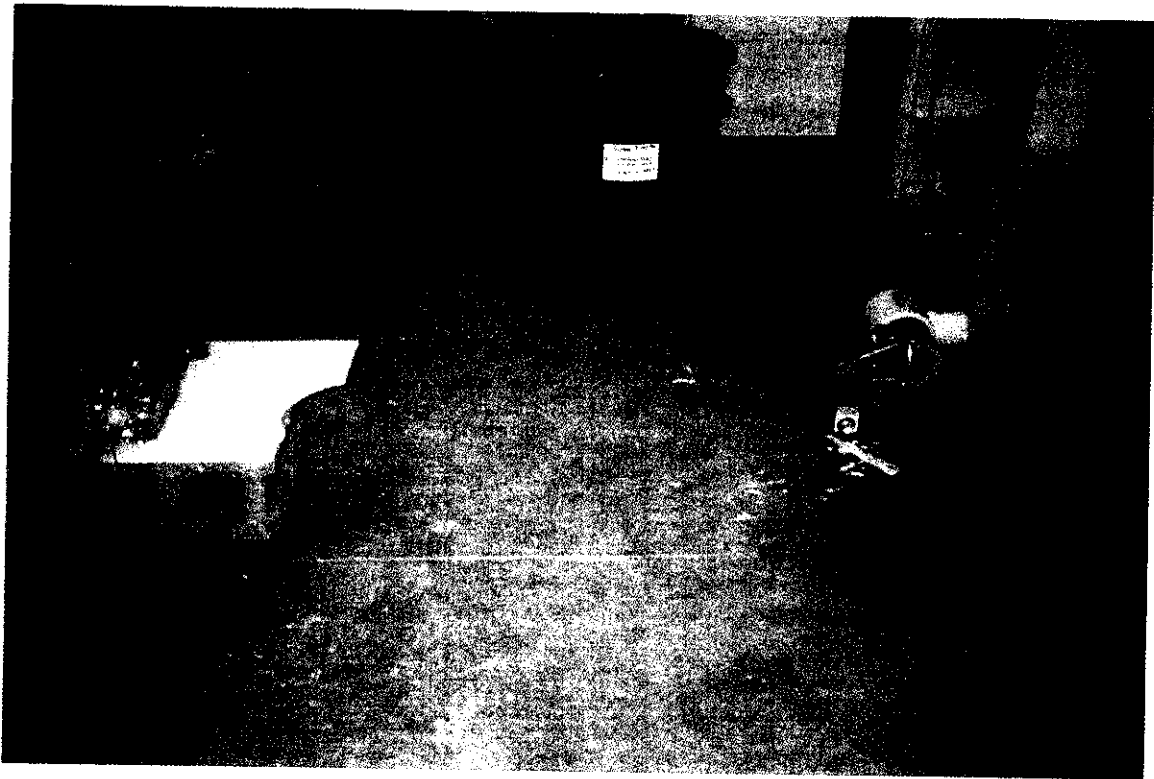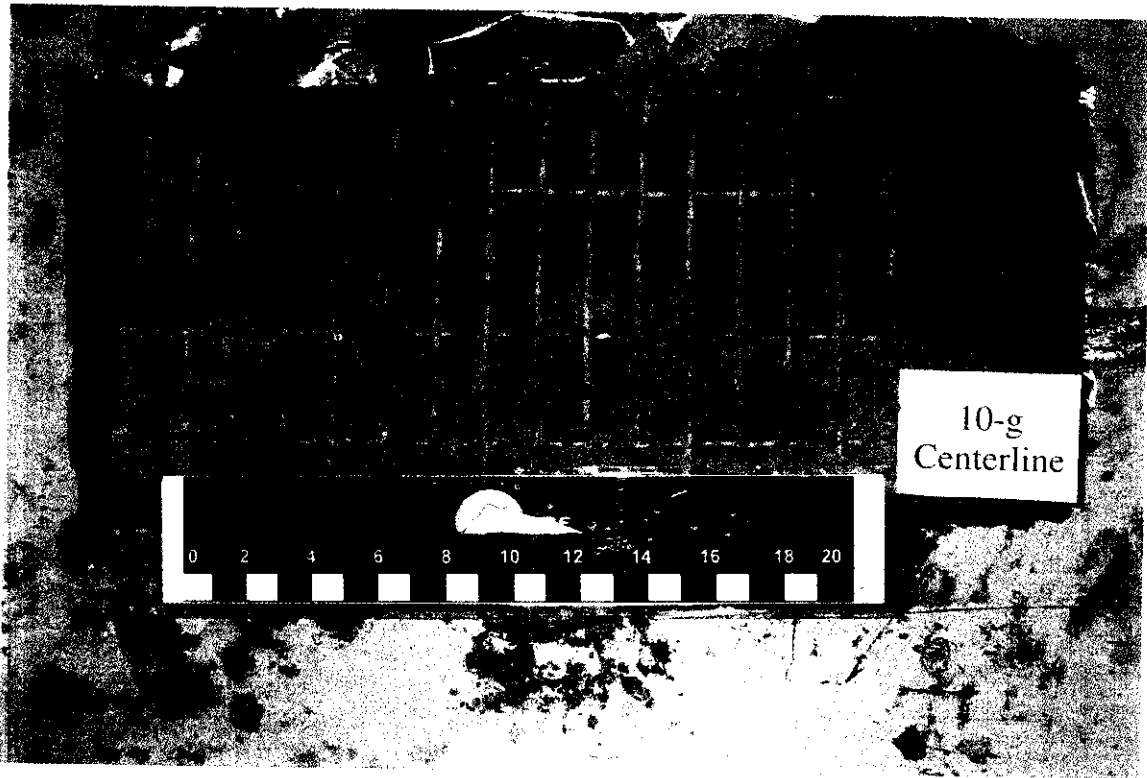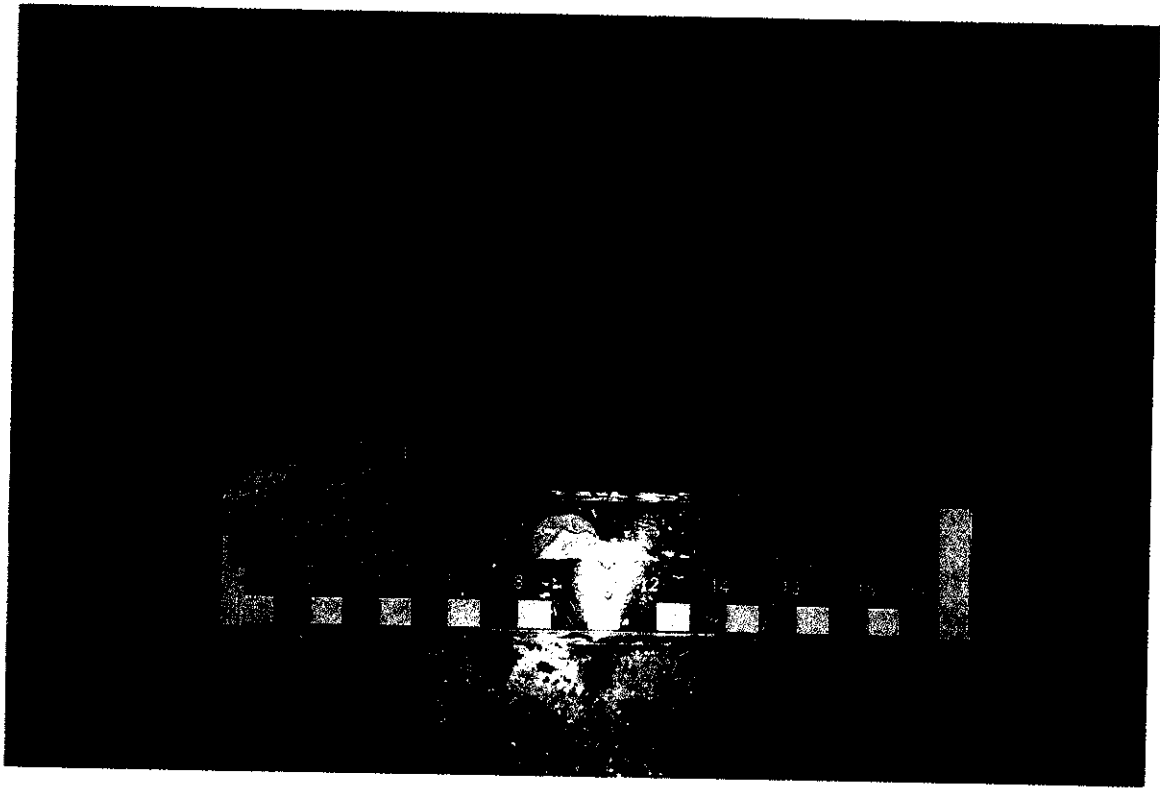|	Photographs of 10-g and 1-g Scours	FIGURE 17

**X-Ray Source and
Sample with Film Canister**

FIGURE
18

	Sample in Position for X-Ray	FIGURE 19

10-g
Centerline

| C-CORE | Grids from 10-g Scour | FIGURE 20 |

1-g
Normal

0 2 4 6 8 10 12 14 16 18 20

1-g
Centerline
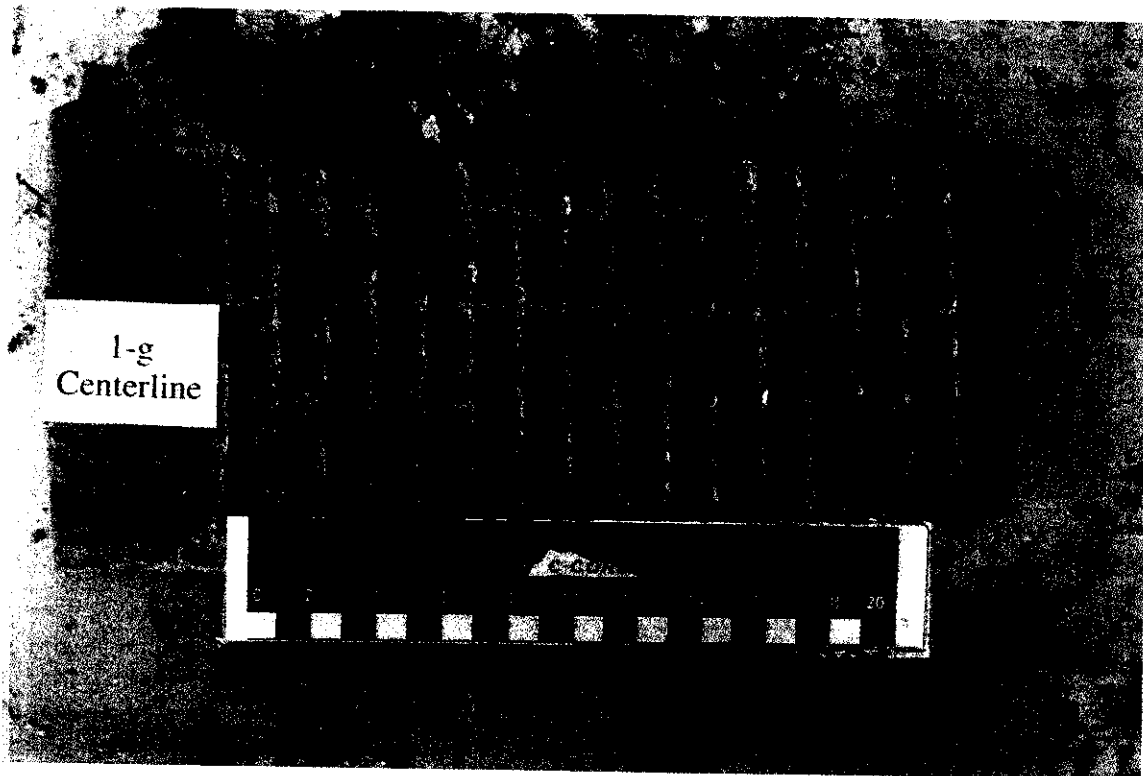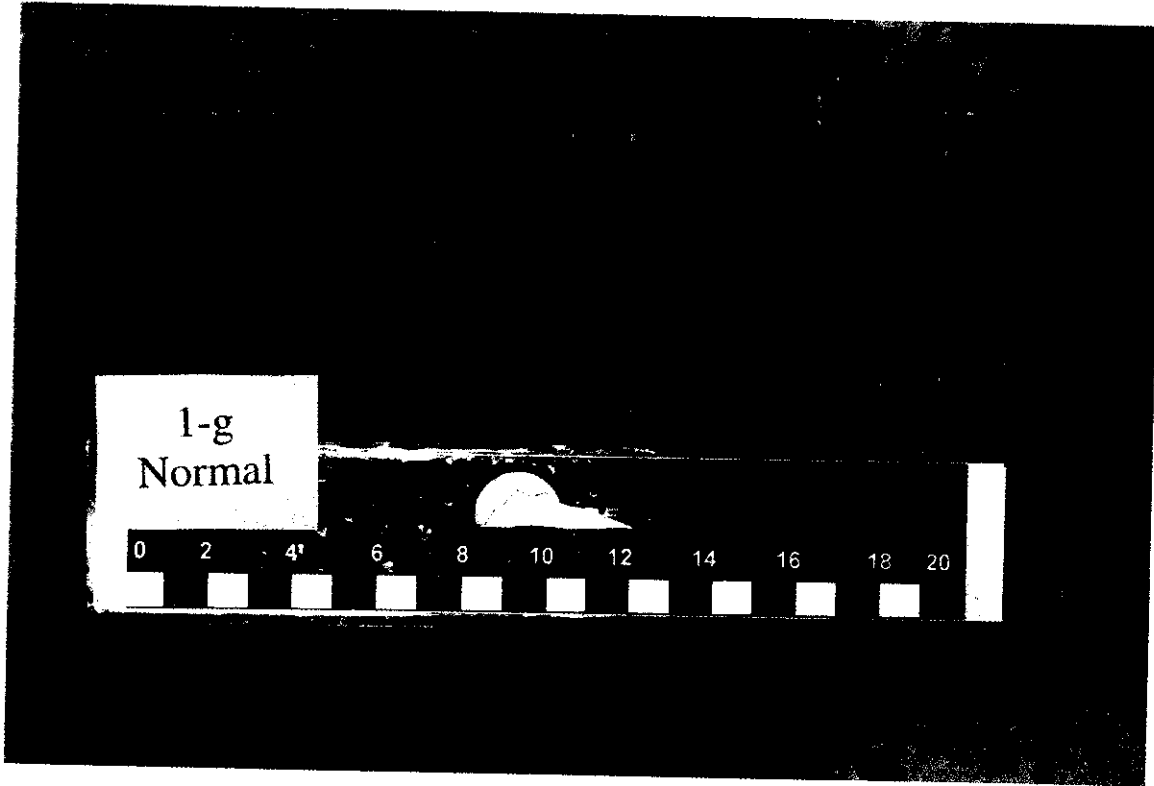
| C-CORE | Grids from 1-g Scour | FIGURE 21 |

30

Profiles
16 & 17

Profiles
18 & 19

x

y

Profile 1 @ 190 mm

Profile 2 @ 250 mm

Profile 3 @ 300 mm

Profile 4 @ 350 mm

Profile 5 @ 400 mm

Profile 6 @ 450 mm

Profile 7 @ 500 mm

Profile 8 @ 550 mm

Profile 9 @ 600 mm

Profile 10 @ 650 mm

Profile 11 @ 700 mm

Profile 12 @ 750 mm

Profile 13 @ 800 mm

Profile 14 @ 850 mm

Profile 15 @ 900 mm

10-G
Scour
@x=245mm

1-G
Scour
@x=695mm
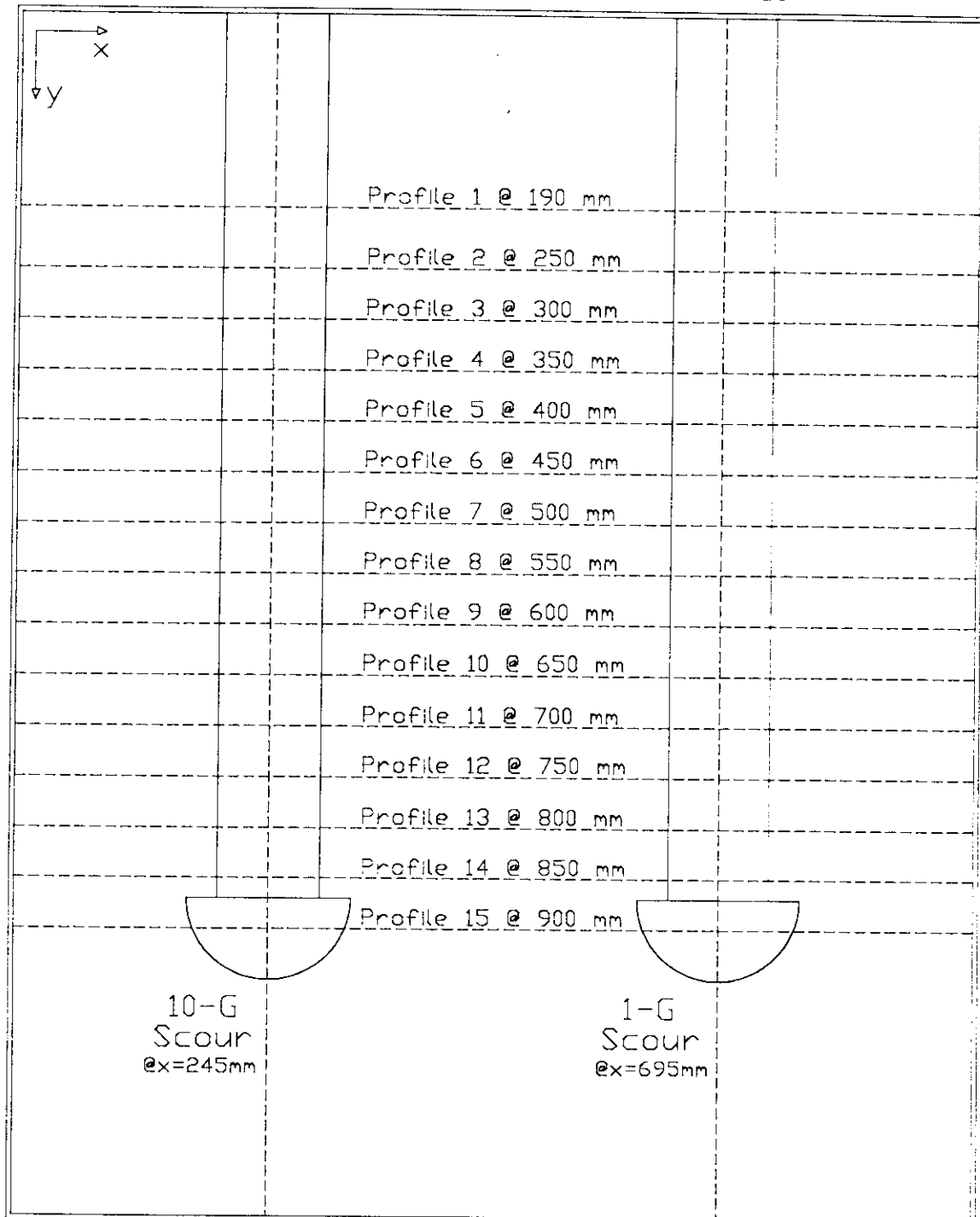
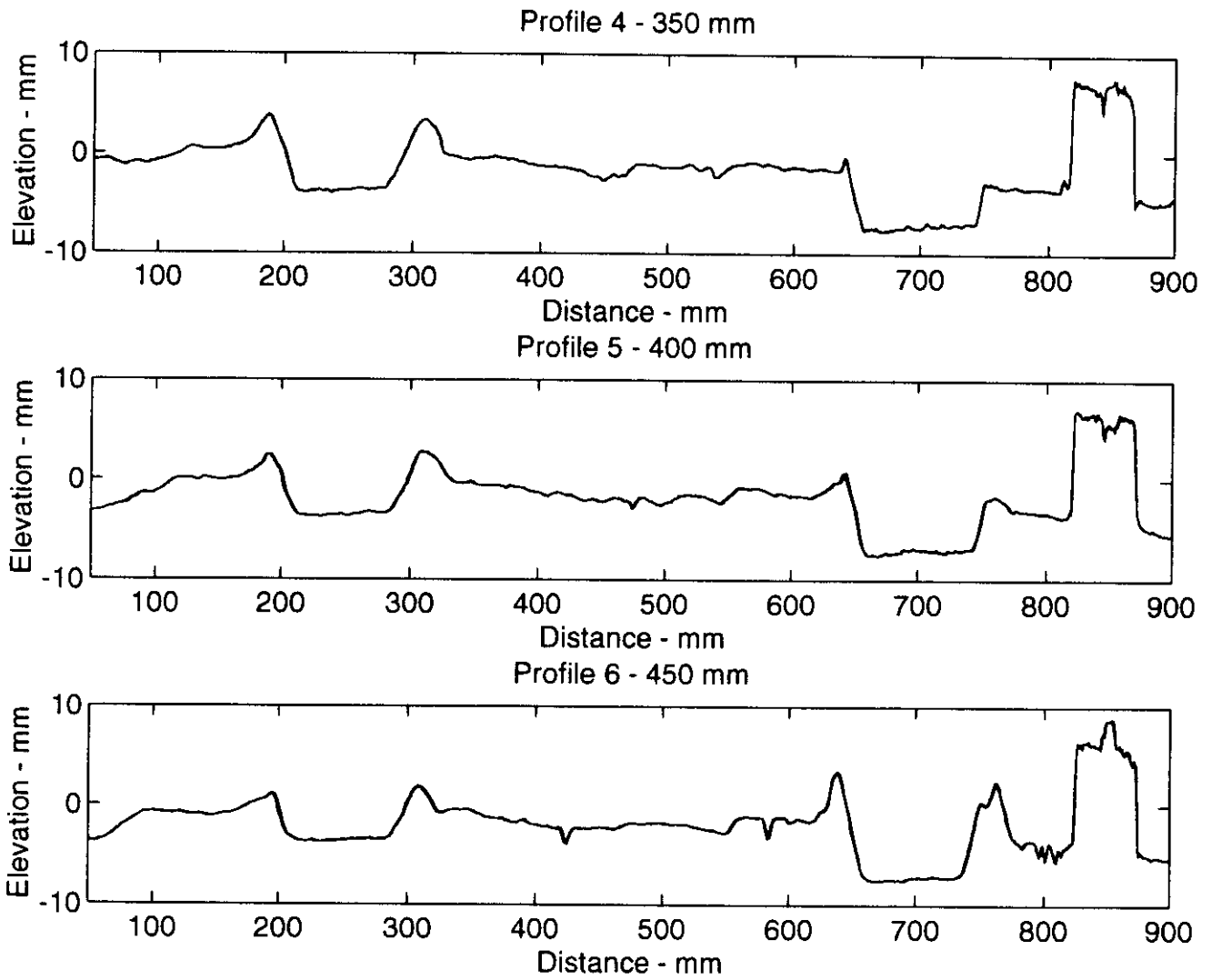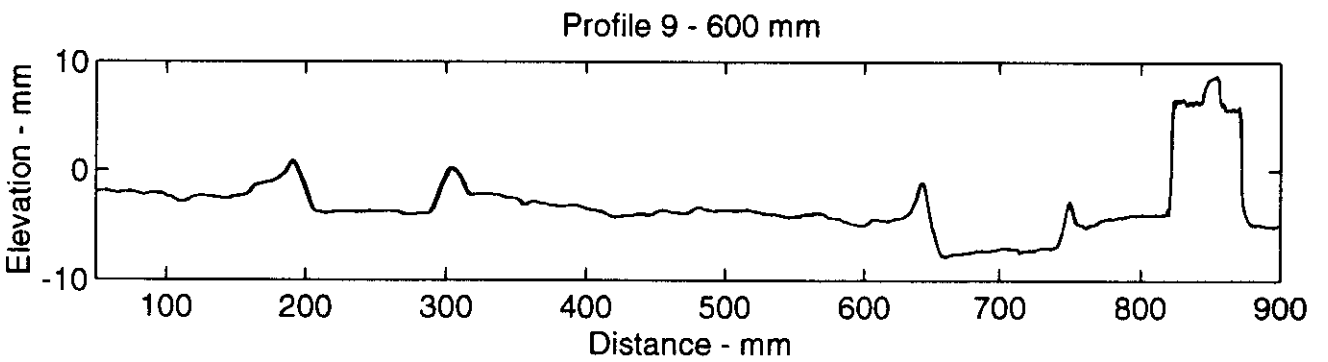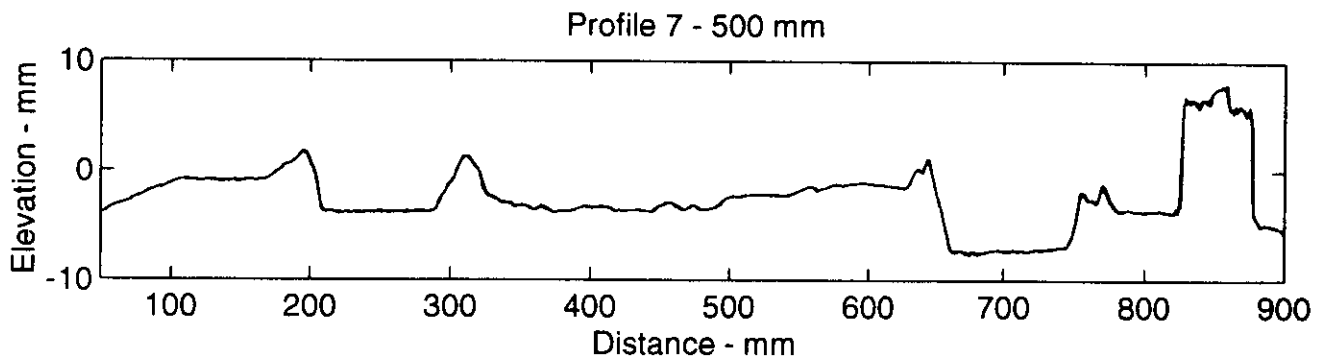|		
C-CORE	**Location of Profiles on Test Package**	**FIGURE** **22**

Profile 1 - 190 mm

Profile 2 - 250 mm
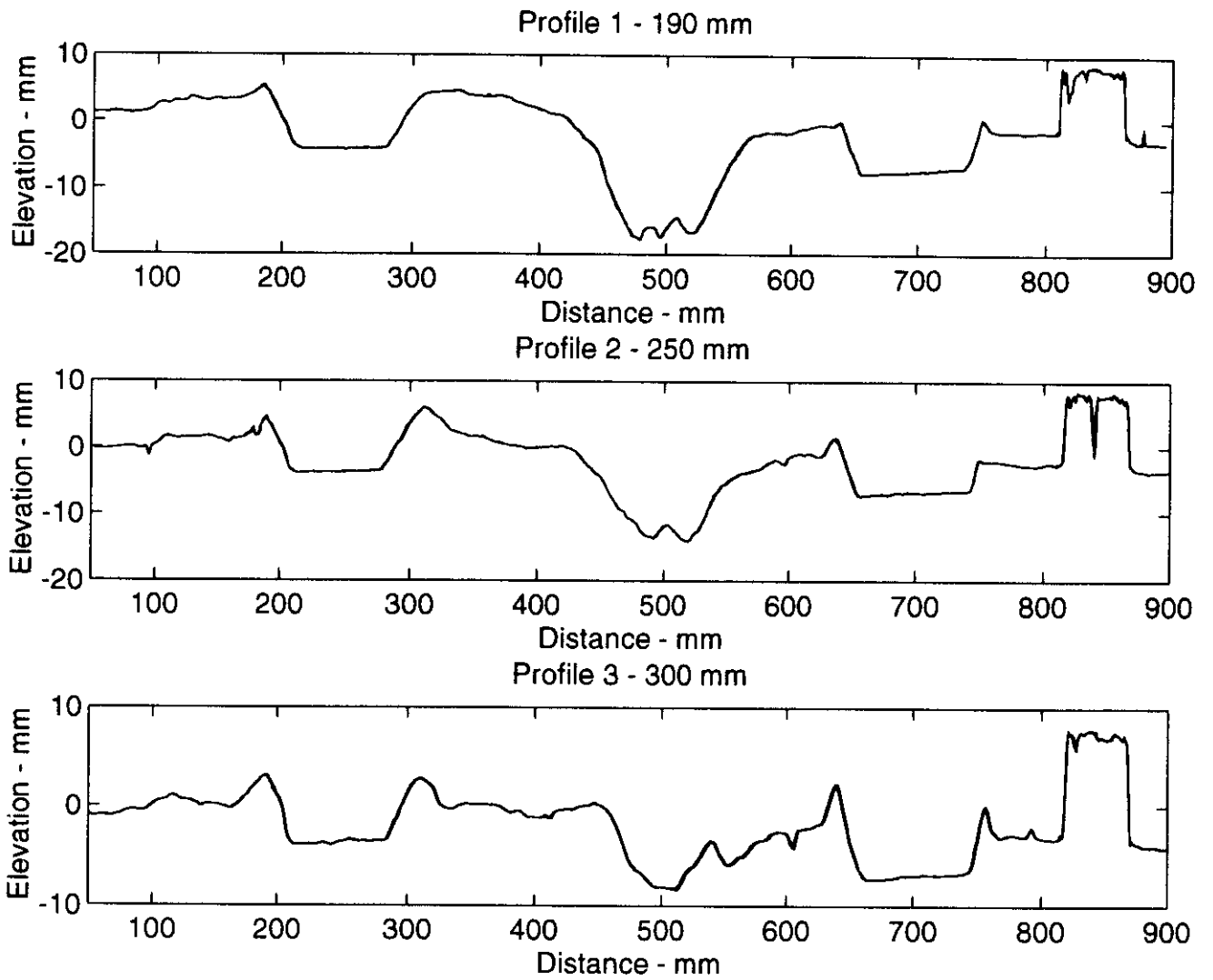
Profile 3 - 300 mm

| | Profiles at Y= 190, 250 and 300 mm | FIGURE 23 |

Profile 4 - 350 mm

Profile 5 - 400 mm

Profile 6 - 450 mm

	Profiles at Y= 350, 400 and 450 mm	FIGURE 24

Profile 7 - 500 mm

Profile 8 - 550 mm
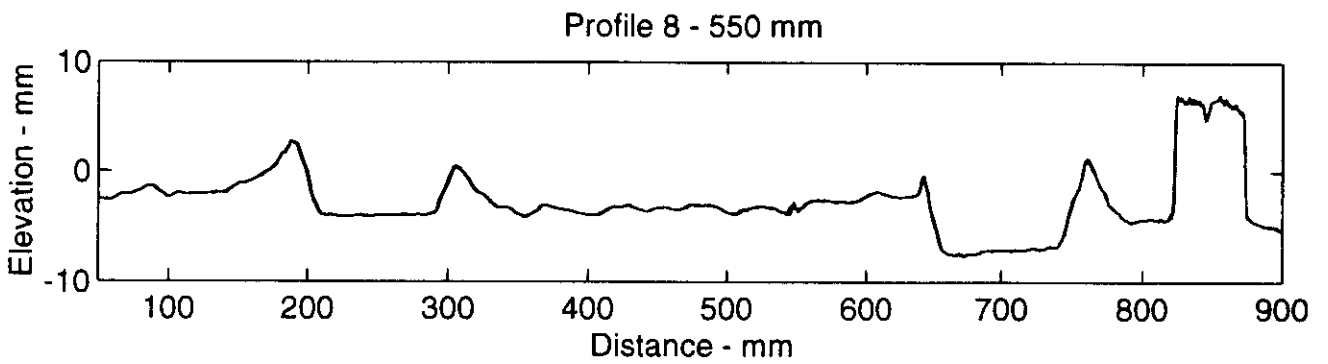
Profile 9 - 600 mm

| | Profiles at Y=
500, 550 and 600 mm | FIGURE
25 |

34

Profile 10 - 650 mm

Profile 11 - 700 mm

Profile 12 - 750 mm
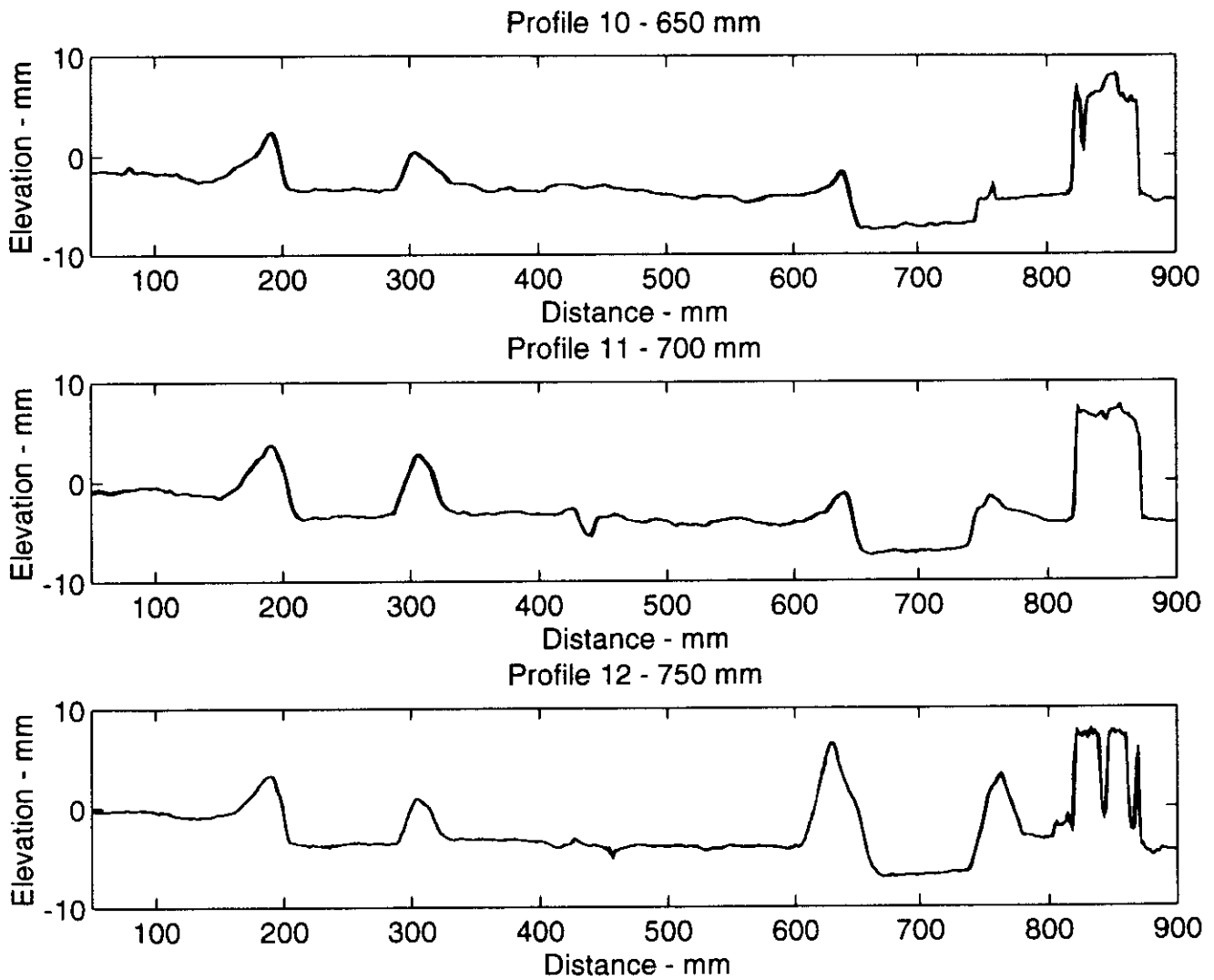
	Profiles at Y= 650, 700 and 750 mm	FIGURE 26

Profile 13 - 800 mm

Profile 14 - 850 mm

Profile 15 - 900 mm
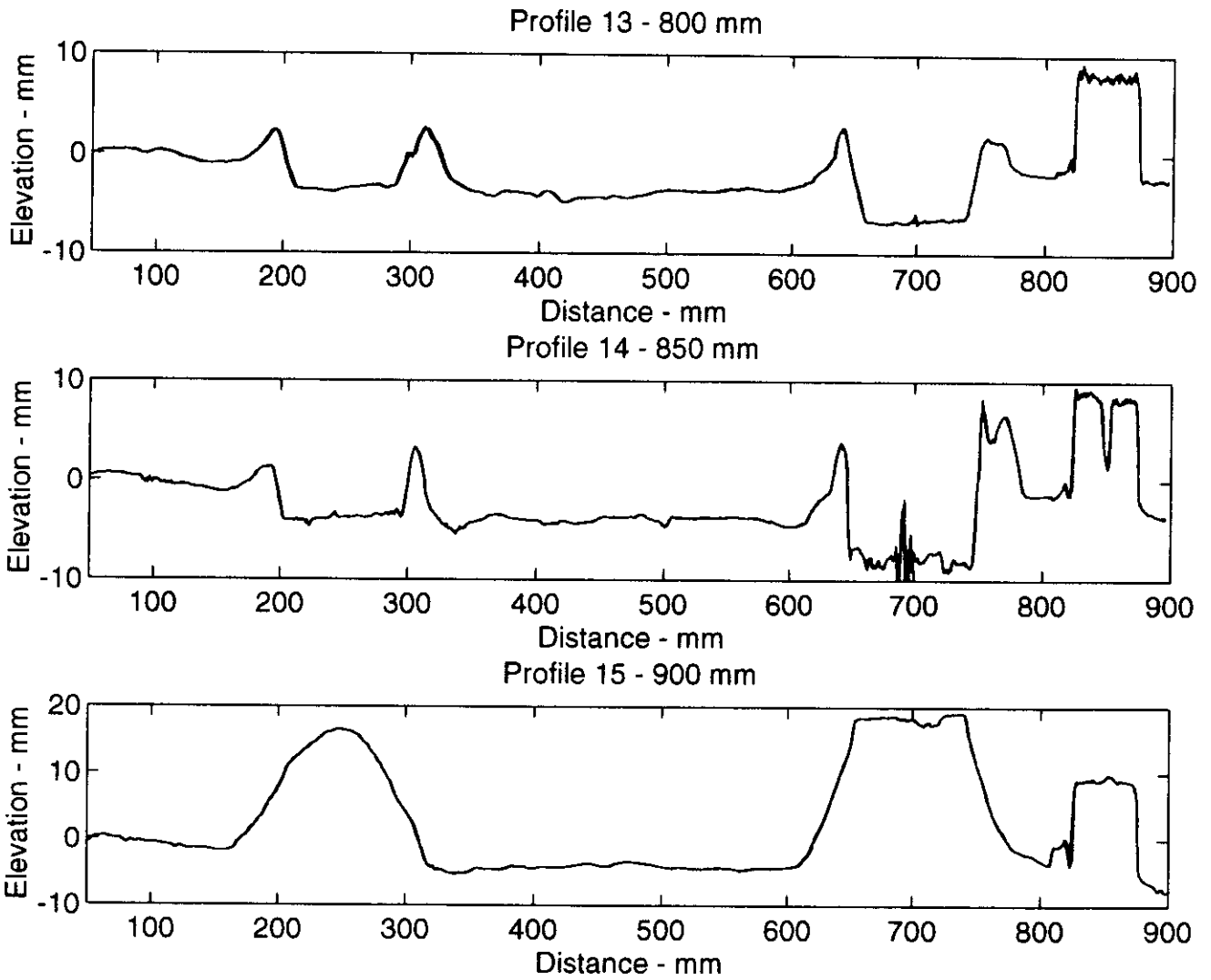
| | Profiles at Y=
800, 850 and 900 mm | FIGURE
27 |

Profile 16 - Along 10-g Scour

Profile 17 - Along 10-g Scour
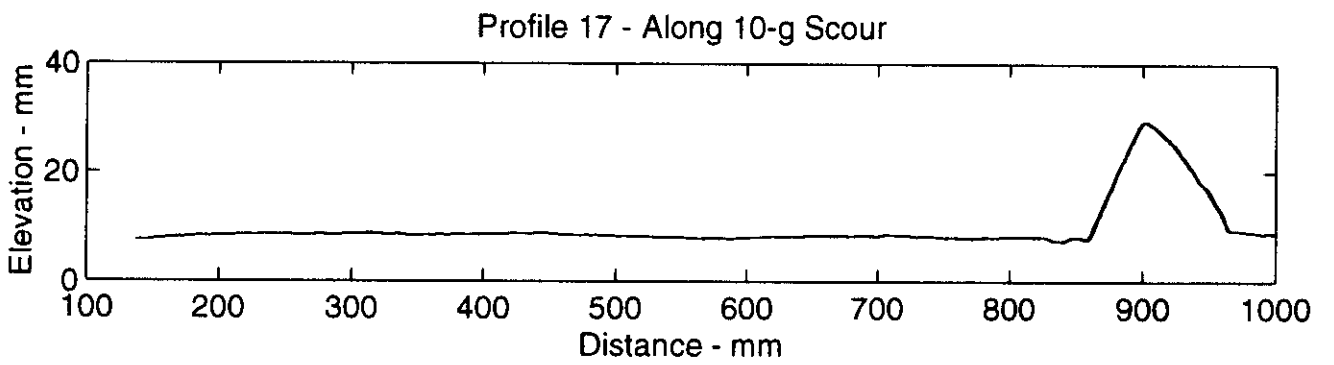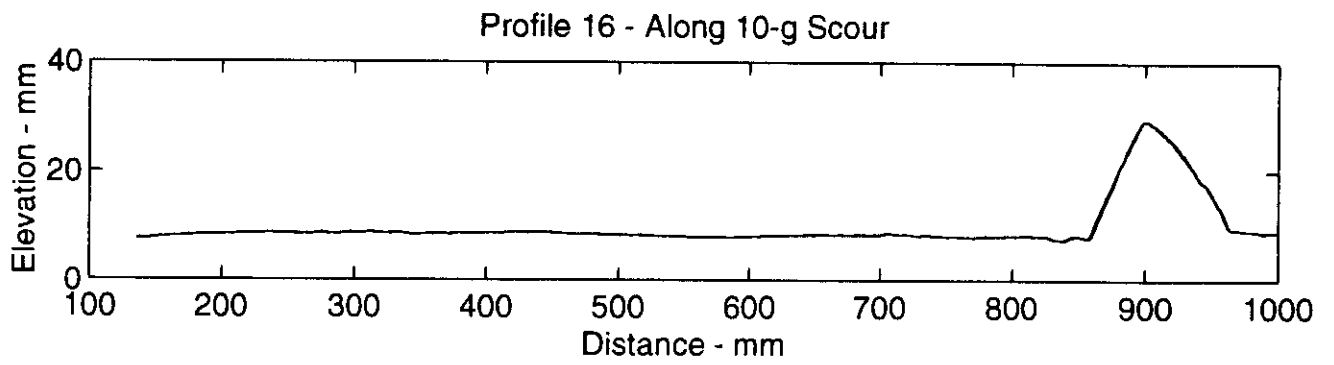
| | Profiles along 10-g Scour | FIGURE 28 |

Profile 18 - Along 1-g Scour

Profile 19 - Along 1-g Scour
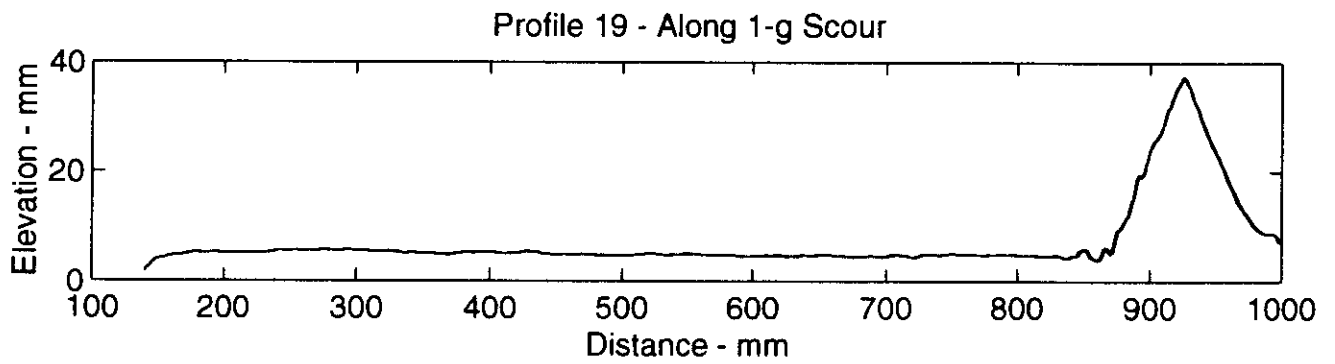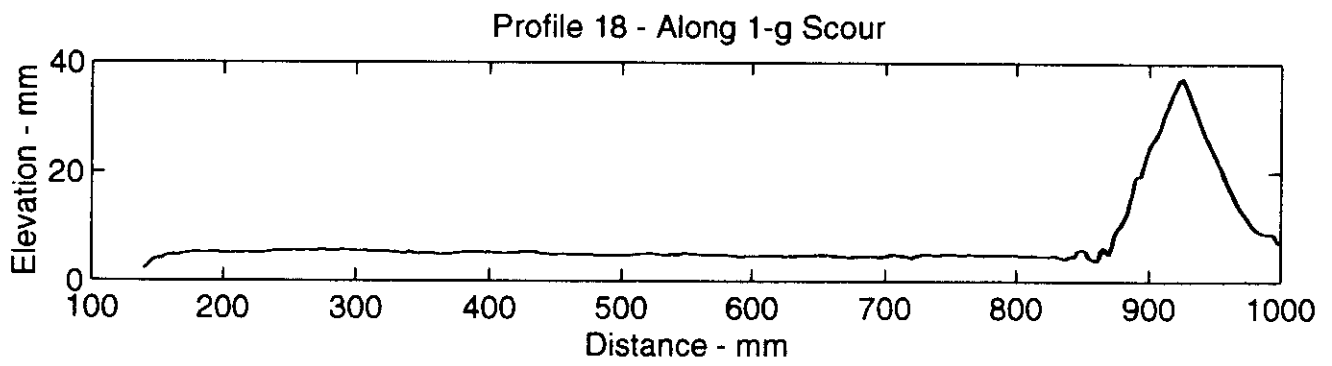
	Profiles along 1-g Scour	FIGURE 29

Table 3.   Scour Depths at Profile Locations

| Profile Location (mm)	10-g Scour Depth (mm)	1-g Scour Depth (mm)
190	7.6	5.7
250	5.3	4.8
300	5.9	6.4
350	5.8	7.0
400	5.0	7.0
450	4.4	7.0
500	3.5	7.0
550	2.5	5.8
600	2.4	4.0
650	1.2	4.4
700	1.8	4.4
750	2.1	4.9
800	1.9	6.3
850	1.9	7.5

6.2 Sub-Scour Displacements

Initial attempts to evaluate sub-scour displacements involved placing the x-rays on a light table and tracing the positions of the lead markers, which were easily viewed using this method. It was readily apparent that the positions of the lead markers were not aligned as would have been expected if they had remained attached to the spaghetti strands. In order to obtain better quality information from the x-rays, the services of MUN's photographic facilities were utilized to obtain contact prints. The quality of the contact prints was such that the actual strands of spaghetti could be discerned within the silt. It was obvious from the prints that quite a few of the lead solder markers had shifted with respect to the spaghetti strands, making the markers less effective for evaluating sub-scour soil deformation. The spaghetti was found to have degraded due to biological action which reduced its

39

effectiveness to support the solder strands. The contact prints were digitized using Autocad and a digitizing tablet. The positions of the spaghetti strands were used, rather than the lead solder, since the spaghetti strands provided continuous information, rather than the piecemeal information produced by the lead solder.

Examination of the marker grids normal to the direction of scour revealed very little evidence of deformation, both for the 1-g and 10-g scours. These marker grids are shown in Figures 30 and 31. The centerline grids, parallel to the direction of the scours, revealed more information regarding the sub-scour soil deformation. Sub-scour deformation beneath the 10-g scour extends to approximately 36 mm beneath the bottom of the scour. Sub-scour deformation beneath the 1-g scour appears to extend approximately 38 mm below the bottom of the scour. Digitized marker grids are shown in Figures 32 and 33. Likewise, examination of lateral deformation at the base of the two scours indicates that the soil immediately under the 10-g scour deformed 4.5 mm laterally and the soil immediately under the 1-g scour deformed 4.6 mm laterally.

10-G Scour
Normal Marker Grid

SCALE - MM
0 10 20 30 40 50
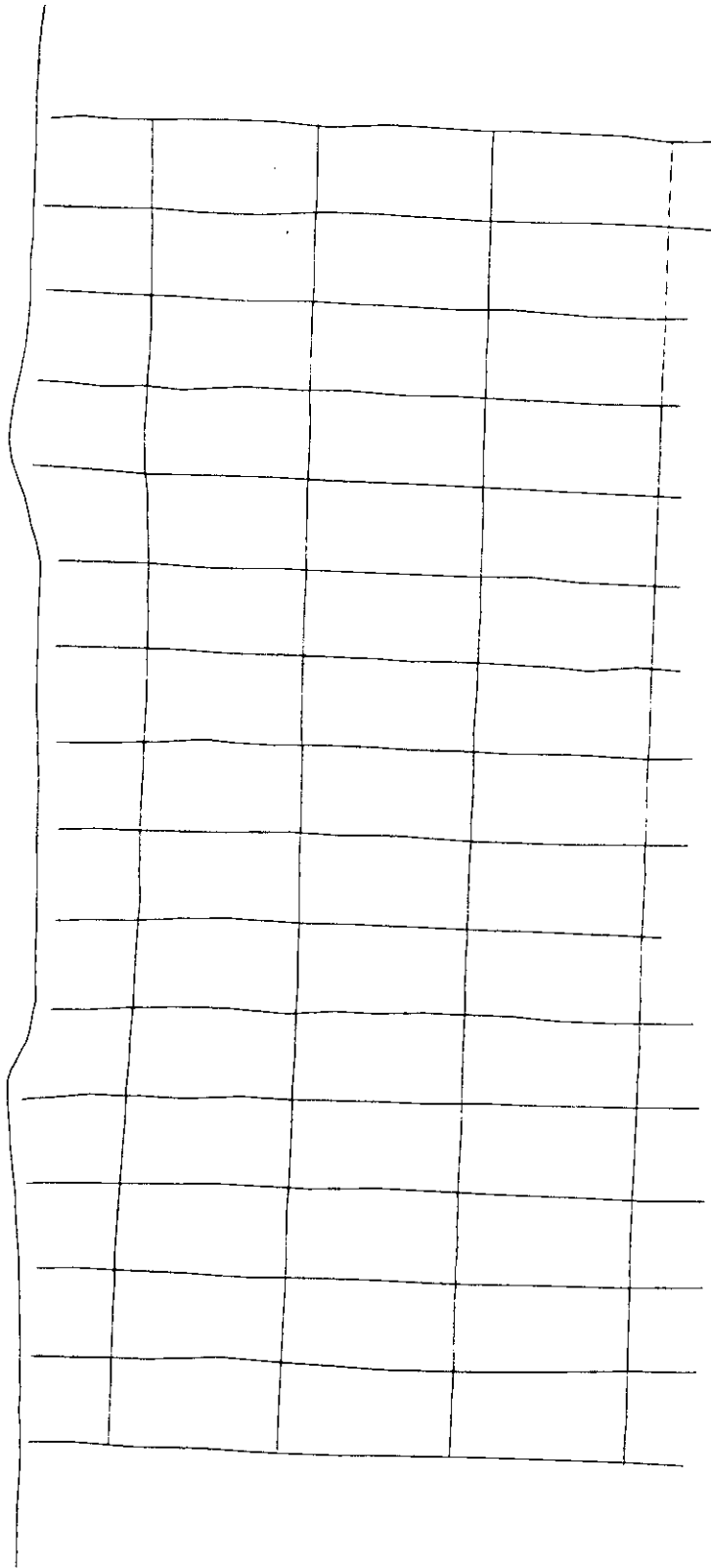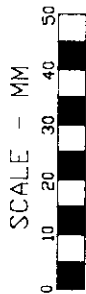
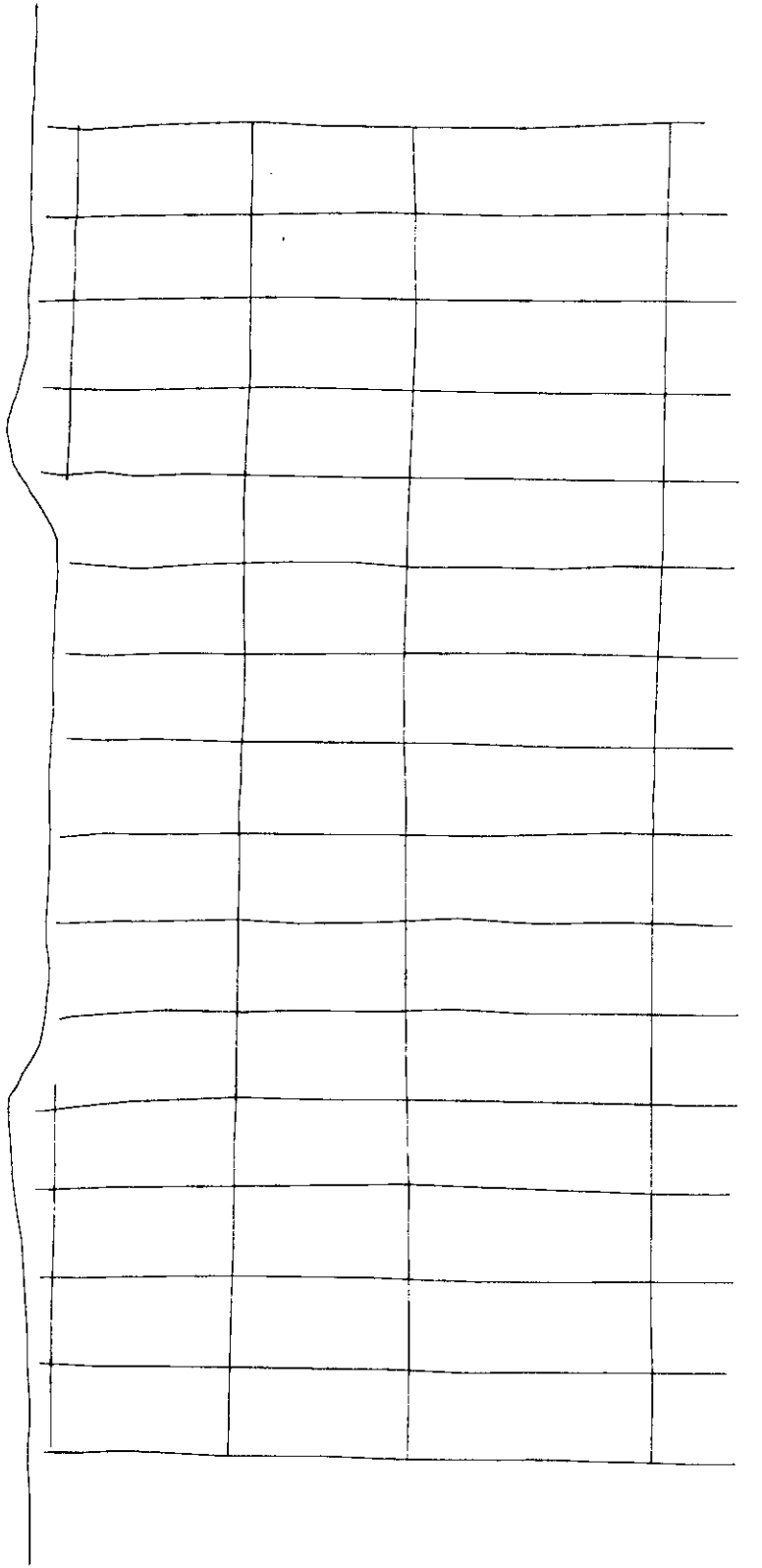|	Grid Normal to 10-g Scour	FIGURE
C-CORE	Digitized from X-Ray	30

1-G Scour

Normal Marker Grid

SCALE – MM
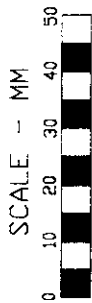
| | Grid Normal to 1-g Scour
Digitized from X-Ray | FIGURE
31 |

10-G Scour
Centerline Marker Grid

SCALE - MM
0 10 20 30 40 50
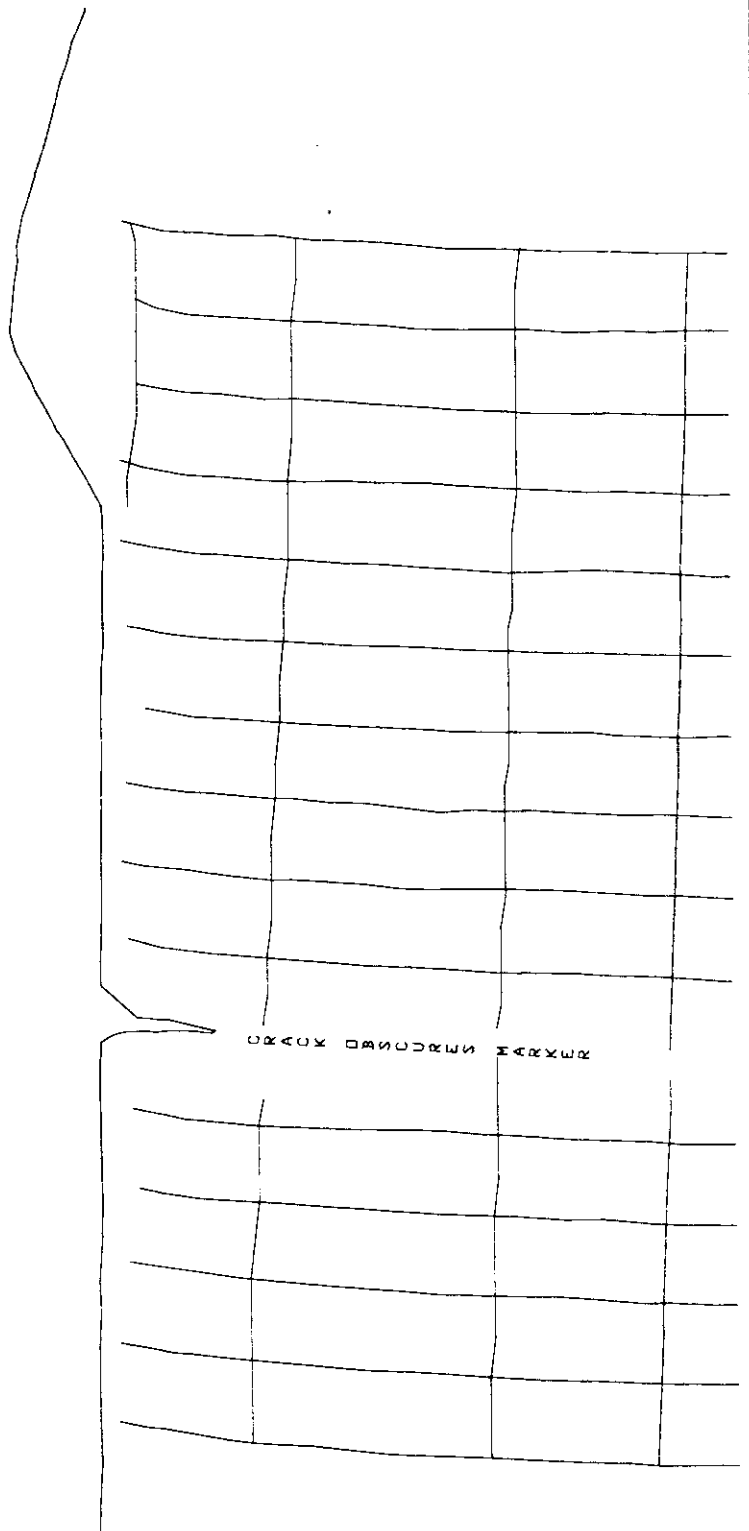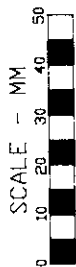
CRACK OBSCURES MARKER

	Centerline Grid From 10-g Scour Digitized from X-Ray	FIGURE
C-CORE		32

1-G SCOUR

Centerline Marker Grid

SCALE - MM
0 10 20 30 40 50
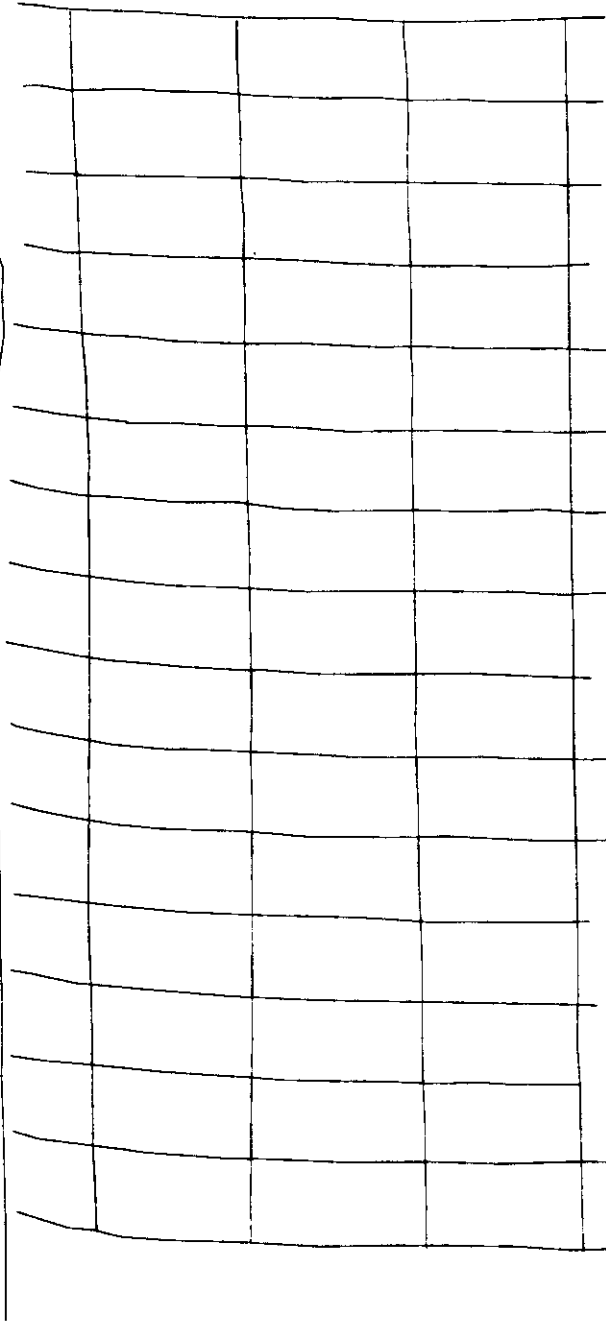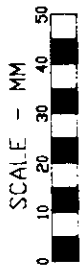
| | Centerline Grid From 1-g Scour Digitized from X-Ray | FIGURE 33 |

C-CORE

44

7.0   ANALYSIS OF 1-G AND 10-G TEST DATA

7.1 Comparison of Sub-Scour Displacements

The deformation depths were normalized with respect to the scour depths, to allow comparison between the two tests. The ratio of deformation depth to scour depth for the 10-g scour is (36 mm)/(3.7 mm) = 9.7. The ratio of deformation depth to scour depth for the 1-g scour is (38mm)/(5.9 mm) = 6.4. Other scour tests conducted at 1-g in low-strength silts (Poorooshasb and Clark, 1990) have indicated deformation depth/scour depths ratio of up to seven.

The lateral deformations at the base of the scour were also normalized with respect to the scour depths. The lateral deformations at the base of the scour are 4.6 and 4.5 mm for the 1-g and 10-g test, respectively. This provides a lateral deformation/scour depth ratio of 1.2 for the 10-g test and a ratio of 0.78 for the 1-g test. The deformations ratios (deformation depth/scour depth and lateral deformation/scour depth) observed for both of these tests are consistent with the sand data presented by Paulin (1992) and in C-CORE report 97-C34 (Clark *et al.*,1997).

7.2 Force Comparison

One parameter that may be used to analyse scour force data is to consider the ratio of the vertical force to the horizontal force (ξ). In previous studies, silts and clays exhibited values of around 2 for ξ, while scour tests in sand had force ratios of about unity. The results for these tests are summarized in the following table.

Table 4.   Force Ratio Parameters for Test PR3d-2

	10-g Scour	1-g Scour
Mean Steady State Vertical Force*, kN	0.58	1.02
Mean Steady State Horizontal Force , kN	0.45	0.68
Force Ratio, ξ	1.3	1.5

* vertical forces had to be estimated due to a equipment malfunction.

A further comparison with previous test data may be made by normalizing the horizontal forces. Two different relationships may be used. For silts and clays, the normalized horizontal force may be calculated using F_h/DBC_u, where F_h is the mean steady-state horizontal force, D is the depth of the scour and C_u is the shear strength of the soil. The results for these tests are given in Table 5.

Table 5.   Normalized Horizontal Forces for Test PR3d-2

	10-g Scour	1-g Scour
Mean Steady State Horizontal Force - kN	0.45	0.68
Scour Depth, D - metres	0.0037	0.0059
Scour Width, B - metres	0.1	0.1
Shear Strength, C_u - kPa	40	40
Normalized Horizontal Force	30.4	28.8

The normalized horizontal forces are quite consistent and are in the range expected for fine-grained soils, as may be seen in Figure 5 of C-CORE report 97-C34.

In both the 1-g and 10-g scour cyclic components can be seen in both the vertical and horizontal loads. This feature is common in scour events and has been reported both in 1-g large scale model scour and scours modelled in the geotechnical centrifuge.

8.0   SUMMARY AND CONCLUSIONS

The second centrifuge test of PRISE Phase 3d was conducted in a saturated dilatant silt at an acceleration of 10-g, on Friday, April 22, 1998. An additional test was also conducted at 1-g for comparison.   The silt used for this test was obtained from the settling pond of a local quarry operation. The model keel used for the tests had a width of 100 mm and an angle of attack of 30°. The model keel was moved at a mean speed of 111 mm/s during the two scour events.

Data were acquired during the test regarding the motion of the keel, lateral and vertical forces on the model keel, contact forces on the keel surface, and excess pore pressures generated in the silt beneath the keel. Post test data were collected via surface profiles, photographic records and x-rays.

The differences between the 10-g and 1-g sub-scour deformations were consistent with what would be expected with the soil stresses induced by increased g-levels. Both the ratio of vertical and horizontal forces observed during the scours, and the normalized horizontal forces, were consistent with what would be expected for a fine-grained silt material.

9.0 REFERENCES

Clark, J., Philips, R., and Winsor, R. (1997). Pressure Ridge Ice Scour Experiment (PRISE) Phase 3c: Extreme Ice Scour Event Modelling and Interpretation, August, C-CORE Publication 97-C34.

Hurley, S., and Phillips, R. (1998). Safety and Integrity of Arctic Marine Pipelines; Progress Report #2 - Centrifuge Test PR3d-1 Report. Contract Report for Minerals Management Service, United States Department of the Interior, C-CORE Publication 98-C2, March.

Paulin, M.J. (1992). Physical Model Analysis of Iceberg Scour in Dry and Submerged Sand. M.Eng. Thesis, Faculty of Engineering and Applied Science, Memorial University of Newfoundland, St. John's, NF.

Paulin, M.J. (1997). Safety and Integrity of Arctic Marine Pipelines; Progress Report #1 - Results of Field Study . Contract Report for Minerals Management Service, United States Department of the Interior, C-CORE Publication 97-C30, July.

Poorooshasb, F. (1989). Large Scale Laboratory Tests of Seabed Scour . Contract Report for Fleet Technology Ltd., C-CORE Publication 89-C15.

Poorooshasb, F. and Clark, J.I. (1990) On Small Scale Ice Scour Modelling , Workshop on Ice Scouring and the Design of Offshore Pipelines. Calgary, Alberta, April 18-19, pp. 193-235.

Pressure Ridge Ice Scour Experiment (PRISE) Phase 3: Centrifuge Modelling of Ice Keel Scour: Draft Final Report. April 1995.